Global Biogeochemical Cycles

RESEARCH ARTICLE
10.1029/2020GB006916

Continental and Ecoregion-Specific Drivers of Atmospheric NO_2 and NH_3 Seasonality Over Africa Revealed by Satellite Observations

Jonathan E. Hickman[1], Niels Andela[2,3], Kostas Tsigaridis[1,4], Corinne Galy-Lacaux[5], Money Ossohou[6], Enrico Dammers[7,8], Martin Van Damme[9], Lieven Clarisse[9], and Susanne E. Bauer[1]

[1]NASA Goddard Institute for Space Studies, New York, NY, USA, [2]Biospheric Sciences Laboratory, NASA Goddard Space Flight Center, Greenbelt, MD, USA, [3]Now at School of Earth and Environmental Sciences, Cardiff University, Wales, UK, [4]Center for Climate Systems Research, Columbia University, New York, NY, USA, [5]Laboratoire d'Aérologie, Université Toulouse III Paul Sabatier/CNRS, Toulouse, France, [6]Laboratoire de Physique de l'Atmosphère et de Mécanique des Fluides, Université Félix Houphouët-Boigny, Abidjan, Côte d'Ivoire, [7]Air Quality Research Division, Environment and Climate Change Canada, Toronto, Canada, [8]Now at Climate, Air and Sustainability, Netherlands Organization for Applied Scientific Research (TNO), Utrecht, The Netherlands, [9]Université libre de Bruxelles (ULB), Service de Chimie Quantique et Photophysique, Atmospheric Spectroscopy, Brussels, Belgium

Abstract

Ammonia (NH_3) and nitrogen oxides (NO_x: nitrogen dioxide [NO_2] + nitric oxide [NO]) play important roles in atmospheric chemistry. Throughout most of Africa, emissions of these gases are predominantly from soils and biomass burning. Here we use observations of tropospheric NO_2 vertical column densities (VCDs) from the Ozone Monitoring Instrument from 2005 through 2017 and atmospheric NH_3 VCDs from the Infrared Atmospheric Sounding Interferometer from 2008 through 2017 to evaluate seasonal variation of NO_2 and NH_3 VCDs across Africa and in seven African ecoregions. In regions where mean annual precipitation (MAP) is under 500 mm yr^{-1}, we find that NO_2 and NH_3 VCDs are positively related to monthly precipitation, and where MAP is between 500 and 1,750 mm yr^{-1} or higher, NO_2 VCDs are negatively related to monthly precipitation. In dry ecoregions, temperature and precipitation were important predictors of NH_3 and NO_2 VCDs, likely related to variation in soil emissions. In mesic ecoregions, monthly NO_2 VCDs were strongly related to burned area, suggesting that biomass burning drives seasonality. NH_3 VCDs in mesic ecoregions were positively related to both monthly temperature and monthly carbon monoxide (CO) VCDs, suggesting that a mixture of soil and biomass burning emissions influenced NH_3 seasonality. In northern mesic ecoregions, monthly temperature explained most of the variance in monthly NH_3 VCDs, suggesting that soil sources, including animal excreta, determined NH_3 seasonality. In southern mesic ecoregions, monthly CO VCDs explained more variation in NH_3 VCDs than temperature, suggesting that biomass burning may have greater influence over NH_3 seasonality.

Plain Language Summary

Ammonia (NH_3) and nitrogen oxides (NO_x: nitrogen dioxide [NO_2] + nitric oxide [NO]) are gases that are emitted naturally as well as through human activity and contribute to air pollution. Throughout most of Africa, emissions of these gases are primarily from vegetation fires and from microbial activity and chemical transformations in soils. Most ecoregions in Africa experience a distinct dry season and rainy season, with fires occurring during the dry season, and more microbial activity occurring in soils during the rainy season. We used satellite observations of NH_3 and NO_2 concentrations in the atmosphere to understand how and why concentrations of these gases vary seasonally across seven distinct African ecoregions. Overall, we find that in dry ecoregions, NO_2 and NH_3 concentrations increase during the rainy season, when increases in precipitation and temperature stimulate greater soil microbial activity and increase emissions of both gases from soils. In contrast, in wetter ecoregions, NO_2 and NH_3 concentrations increase during the dry season. The increase in NO_2 concentrations is a result of the increase in vegetation fires during this time of the year, but NH_3 concentrations increase due to seasonal changes in both soil and fire emissions.

Key Points:

- For mean annual precipitation (MAP) below 500 mm yr^{-1}, monthly gas concentrations were positively related to monthly precipitation
- For MAP between 500 and 1,750 mm yr^{-1}, monthly nitrogen dioxide (NO_2) was negatively and monthly ammonia (NH_3) was unrelated to monthly precipitation
- The importance of soil and biomass burning for NO_2 and NH_3 seasonality varied across biomes depending on rainfall and other characteristics

Supporting Information:

Supporting Information may be found in the online version of this article.

Correspondence to:

J. E. Hickman,
jonathan.e.hickman@nasa.gov

Citation:

Hickman, J. E., Andela, N., Tsigaridis, K., Galy-Lacaux, C., Ossohou, M., Dammers, E., et al. (2021). Continental and ecoregion-specific drivers of atmospheric NO_2 and NH_3 seasonality over Africa revealed by satellite observations. *Global Biogeochemical Cycles*, *35*, e2020GB006916. https://doi.org/10.1029/2020GB006916

Received 14 DEC 2020
Accepted 29 JUN 2021

Author Contributions:

Conceptualization: Jonathan E. Hickman, Niels Andela, Kostas Tsigaridis, Corinne Galy-Lacaux, Money Ossohou, Enrico Dammers, Susanne E. Bauer
Formal analysis: Jonathan E. Hickman
Resources: Martin Van Damme, Lieven Clarisse
Writing – original draft: Jonathan E. Hickman
Writing – review & editing: Jonathan E. Hickman, Niels Andela, Kostas Tsigaridis, Corinne Galy-Lacaux, Money Ossohou, Enrico Dammers, Martin Van Damme, Lieven Clarisse, Susanne E. Bauer

1. Introduction

Reactive nitrogen (N) trace gases—which include ammonia (NH_3) and the nitrogen oxides nitric oxide (NO) and nitrogen dioxide (NO_2)—play a range of important roles in the atmosphere, with implications for human health, climate, and ecosystem functions. Fossil fuel combustion and anthropogenic alterations to soils through fertilization or livestock management are the primary sources of these gases in many parts of the world, but emissions from natural soils and biomass burning can also be important sources, particularly in regions with relatively low fossil fuel combustion and fertilizer use such as Africa (Jaeglé et al., 2005). Once in the atmosphere, NH_3 contributes to the production of inorganic aerosols, the primary constituents of fine particulate matter and a serious health hazard (Bauer et al., 2016; Lelieveld et al., 2015; Pope et al., 2002). NH_3 can also be deposited to downwind ecosystems, contributing to eutrophication, soil acidification, vegetation damage, productivity declines, reductions in biodiversity, and indirect greenhouse gas emissions (e.g., Denier Van Der Gon & Bleeker, 2005; Krupa, 2003; Matson et al., 1999; Stevens et al., 2018; Tian & Niu, 2015). Because there is rapid interconversion and equilibration of NO and NO_2 in the atmosphere during the day, they are collectively referred to as NO_x. NO_x is in itself an air pollutant, and is also a key precursor to the formation of tropospheric ozone, which is damaging to both crop productivity and human health; anthropogenic ozone pollution causes roughly half a million premature deaths annually (Silva et al., 2013).

Both NO_x and NH_3 are emitted from a number of the same anthropogenic and natural sources—particularly soils and biomass burning—but there are important differences in the processes responsible for the production and emission of each gas. NO_x emissions include biofuel and fossil fuel combustion, lightning, biogenic NO emissions from soils, and biomass burning. NH_3 can be produced abiotically from ammonium (NH_4^+) in soils, fertilizer, and animal excreta, during biomass burning, and during industrial processes. Globally, the majority of NO_x emissions are from fossil fuel combustion, and although that is also the case in South Africa, in equatorial Africa it is a minor source (Jaeglé et al., 2005). Instead, biogenic soil sources dominate NO_x emissions in northern hemisphere equatorial Africa with most of the remaining NO_x emissions coming from biomass burning, with the reverse being true in southern hemisphere equatorial Africa (Jaeglé et al., 2005), and fossil fuel emissions are a growing but still relatively minor source over Africa and unlikely to contribute to seasonal changes in atmospheric composition (Hickman et al., 2021; Hoesly et al., 2017; Jaeglé et al., 2005; van der A et al., 2008). That may change in the future, as fossil fuel combustion emissions of NO_x are expected to increase by up to a factor of 6 as a result of the rapid growth in the adoption of two-stroke motors, conceivably becoming the largest source of NO_x in Africa by 2030 (Liousse et al., 2014). Although fossil fuel combustion can be a source of NH_3 when catalyzers are used to limit NO_x emissions, it currently makes a minor contribution to global NH_3 emissions (Behera et al., 2013). Instead, agricultural soils are the primary source of NH_3 globally (Behera et al., 2013; Bouwman et al., 2008), with biomass burning responsible for another fifth of emissions, though this estimate is subject to large uncertainties (Olivier et al., 1998; Sutton et al., 2013). The relatively low fertilizer use (Hazell & Wood, 2008; Masso et al., 2017; Vitousek et al., 2009) and livestock manure N content (Rufino et al., 2006, 2014) in sub-Saharan Africa suggest that natural soils may be a more important source in the region than elsewhere in the world.

1.1. Biomass Burning Emissions

Africa is a major site of biomass burning. About half of the global carbon emissions from fire originate from Africa (van der Werf et al., 2017), and similar proportions of NO_x and NH_3 emissions from fire (Cahoon et al., 1992; Jaeglé et al., 2005; Whitburn et al., 2015). In regions where biomass burning is widespread, it can be the primary determinant of seasonality in NO_x (Adon et al., 2010; Galy-Lacaux & Delon, 2014; van der A et al., 2008) and NH_3 (Whitburn et al., 2015). Biomass burning occurs during the dry seasons—generally from November to February in the fire band in northern hemisphere Africa, and from May to October in the fire band in southern hemisphere Africa. Fires emit more NO_x than NH_3 in tropical savannas: with estimated emission factors of 3.9 g NO_x kg^{-1} dry matter and 0.52 g NH_3 kg^{-1} dry matter, respectively (Akagi et al., 2011), though it is thought that these emission factors may be quite variable through the year as changes in fuel moisture influence combustion efficiency (though the possibility that variation in the N content of fuel contributes to the seasonality of emissions cannot be excluded; Zheng et al., 2018). NO_x emissions from biomass burning result primarily from the oxidation of N in fuel (in contrast to fossil fuel combustion, in which NO_x is also produced from atmospheric N_2 at high temperatures). N in fuel is present

predominantly in a chemically reduced state, and NH_3 can also be emitted under conditions where fuel N is incompletely oxidized. Consequently, NO_x is the dominant reactive N species emitted during higher temperature flaming combustion, whereas NH_3 is the dominant reactive N species emitted during lower temperature smoldering combustion, which is reflected in differences in emission factors between savannas and tropical forests, with the latter having more smoldering combustion (Akagi et al., 2011; Goode et al., 1999; Yokelson et al., 2008). Seasonal variation in fuel moisture content can be an important determinant of biomass burning emissions composition (Chen et al., 2010; van Leeuwen & van der Werf, 2011).

1.2. Soil Emissions

Soils—including those affected by animals and livestock—are important sources of both NO_x (in the form of NO) and NH_3, with Africa responsible for nearly 30% of NO_x emissions from soil globally (Jaeglé et al., 2005). NO is produced biogenically by soil microbes, primarily as an intermediary in nitrification, as well as during denitrification; abiotic production of NO through chemodenitrification represents a relatively minor source (Pilegaard, 2013). NH_3 is produced abiotically through the deprotonation of NH_4^+ according to the following formula:

$$NH_4^+ + OH^- \leftrightarrow NH_3 + H_2O \quad (1)$$

Both nitrification and NH_3 volatilization are regulated by substrate availability, temperature, pH, and soil moisture, all of which vary seasonally. They also both depend on NH_4^+ as a substrate, so biogenic processes such as nitrogen mineralization—which tend to slow down during the dry season and exhibit strong pulses of activity at the onset of the rainy season (Birch, 1958)—can be important mediators of NH_3 and NO emissions from soils. Both processes are also strongly temperature dependent, which can lead to additional seasonality. Nitrification generally has a temperature optimum ranging between 30°C and 35°C, and exhibits clear temperature dependence from 5°C to 35°C (Paul & Clark, 1996; Saad & Conrad, 1993; Seifert, 1980). NH_3 volatilization is also temperature-dependent, doubling with every 5°C increase in temperature, though plant and soil physiological and physical factors can moderate the temperature dependence of the actual NH_3 flux (Sutton et al., 2013).

Seasonal changes in soil moisture can be the primary control over seasonality in nitrification and NH_3 volatilization from soils, especially in regions with distinct dry and rainy seasons. During the dry season, the lack of soil moisture tends to limit production and emission of both gases (Davidson et al., 1991; Delon et al., 2019; Hickman et al., 2017; Soper et al., 2016). In the case of nitrification, increases in soil moisture provide microbes with greater access to substrates in solution and promote population growth. However, when high levels of soil moisture shift soil conditions from aerobic to anaerobic, nitrification rates tend to decrease and denitrification rates to increase (Davidson & Verchot, 2000). Soil anaerobicity would tend to favor the further reduction of NO to N_2O and N_2 via denitrification, and thus reduce the net soil NO flux. Increases in soil moisture can also stimulate soil N mineralization rates (Guntiñas et al., 2012) leading to higher NH_4^+ concentrations, as well as favoring NH_3 volatilization (Al-Kanani et al., 1991; Sommer et al., 2004).

Since soil emissions of NO and NH_3 both increase when N availability is higher, addition of fertilizer can play a large role in the seasonality of both gases in regions where fertilizer use is substantial (e.g., Balasubramanian et al., 2015). Although Egypt uses fertilizer at rates in excess of many European countries, it is an exception among African countries. Instead, fertilizer use is extremely low in the vast majority of African and especially in sub-Saharan African countries (Hazell & Wood, 2008), with many countries applying it at rates of less than 10 kg N ha^{-1} (World Bank, 2019), over an order of magnitude lower than rates typical in the United States or China (Vitousek et al., 2009). Under conditions of low fertilizer use, the timing of fertilizer applications may have relatively little impact on the seasonality of atmospheric N trace gas concentrations.

Livestock excreta are an important source of NH_3 emissions (e.g., Bauer et al., 2016). Livestock densities can be relatively high in parts of Africa, particularly in the northern grassland ecosystems (Robinson et al., 2014). However, some factors may make these somewhat lower sources of NH_3 than equivalent densities of livestock elsewhere in the world. First, much livestock production in Africa takes place in pastoral or agropastoral contexts, which limits manure storage and the time over which NH_3 can volatilize from the manure. Second, manure N content is highly variable and often low (Paul et al., 2017; Rufino

et al., 2006, 2014; Vanlauwe & Giller, 2006), limiting the substrate available for NH_3 volatilization. For example, cattle in Sweden have been observed to excrete N at rates 2–6 times higher than cattle in Kenya or Mali (Rufino et al., 2006).

1.3. NO_x and NH_3 Lifetimes and Sinks

In addition to differences in emissions sources, variation in sinks can influence atmospheric NO_x and NH_3 lifetimes and concentrations, but generally this influence only affects seasonal variation in concentrations over industrial areas outside the tropics, where there is little seasonality in emissions (van der A et al., 2008). Lifetimes of both species are short, typically on the order of hours, and change with atmospheric concentrations. The primary sinks of atmospheric NH_3 are dry and wet deposition, so changes in deposition velocities and precipitation can influence atmospheric concentrations: in tropical environments, more frequent rainfall events during the rainy season would tend to decrease NH_3 lifetimes, all else being equal. Reactive losses of NH_3 are also important, so changing concentrations of reactants such as NO_x and sulfur dioxide (SO_2) can influence NH_3 concentrations in the atmosphere (Seinfeld & Pandis, 2016). Globally, the main sink of NO_x is oxidation by hydroxyl radicals (OH) to nitric acid (HNO_3) followed by deposition (Jacob, 1999). But NO_x is also lost through dry deposition, and is involved in a number of chemical transformations, with HNO_3, peroxyacetyl nitrate, peroxynitric acid (HNO_4), alkyl nitrates, and dinitrogen pentoxide ($N2O_5$) potential sinks and sources, and net NO_x chemistry is also influenced by the burden of NO_x in the atmosphere.

1.4. Biomes

The distribution of biomes is well understood to be broadly determined by climate (e.g., Hirota et al., 2011). In Africa, the seasonal migration of the Intertropical Convergence Zone (ITCZ) results in regions with distinct temperature and rainfall seasonality, as well as a latitudinal gradient in rainfall. The geographic distribution of the seasonal distribution and total amounts of rainfall has resulted in the development of a range of different ecoregions within Africa, each with distinct vegetation cover and levels of primary productivity. These include dry savanna, wet savanna, forest-savanna mosaics, forest, and Miombo woodlands. The magnitude and seasonality of temperature and precipitation—including in how they mediate net primary productivity—are also the primary determinants of the fire regime within ecoregions (Krawchuk et al., 2009). Since precipitation, temperature, primary productivity, and fire regime—all of which are important determinants of biogeochemical cycling (e.g., Reich et al., 2001; Vitousek, 2004)—vary across biomes, the seasonality of N cycling, and of NO_x and NH_3 emissions, would be expected to vary across African ecoregions as well.

1.5. Objectives

Atmospheric concentrations of NO_x and NH_3 can undergo substantial seasonal variation in many parts of the world. These gases are important air pollutants, and understanding how they vary seasonally—as well as insight into what causes that seasonal variation—can provide researchers and decision makers with information that can help them understand how, where, and when emissions may need to be better managed to mitigate pollution episodes. These gases also represent important loss pathways of N from ecosystems as well as sources for deposition of N; understanding their seasonality can provide additional insight into the N cycle in these ecosystems. Relative to other parts of the world, biogeochemical cycling and trace N gases in sub-Saharan Africa have been under-studied. A systematic analysis of the seasonality of reactive trace N gases at the continental scale, as well as using an ecoregion perspective, can provide insights into the seasonal dynamics of the biogeochemical processes underlying their emission.

In the last two decades, there has been increased scientific understanding of the magnitude and sources of emissions of trace N gases from Africa due in part to the development of space-borne remote-sensing instruments. These instruments have been used to evaluate seasonality of NO_2 and NH_3 vertical column densities (VCDs). Earlier studies in Africa have evaluated seasonality of NH_3 and NO_2 at the site scale (e.g., Adon et al., 2010; Delon et al., 2010; Ossohou et al., 2019) or in relation to emission sources such as biomass burning in productive savannas or pulsed emissions from soils in the Sahel at regional scales (Hickman et al., 2018; Jaeglé et al., 2004; Whitburn et al., 2015), but a systematic evaluation of seasonality in these

gases for the continent has not been conducted. In regions with substantial biomass burning, the seasonality of burning has been closely associated with the seasonality of NO_2 emissions and concentrations (Jaeglé et al., 2005; Ossohou et al., 2019; van der A et al., 2008). The seasonality of burning has also been associated to some extent with NH_3 concentrations and emissions, though unlike in other world biomass burning regions, seasonal changes in NH_3 concentrations lag 1–2 months behind seasonal changes in fire radiative power in Africa, suggesting that additional sources are important determinants of seasonality (Whitburn et al., 2015). In less vegetated regions of Africa with distinct seasonality in precipitation, seasonal variation in soil emissions of NO (Delon et al., 2012; Ghude et al., 2008; Hudman et al., 2012; Jaeglé et al., 2004, 2005) and NH_3 (Hickman et al., 2018) appears to be a key driver of seasonal changes in the atmospheric concentrations of both gases. Here we build on these previous efforts by using multiple satellite remote-sensing products and spatial data sets to explore the various controls over spatio-temporal variation in both NO_2 and NH_3 VCDs in Africa, identify how mean annual precipitation (MAP) determines where soil emissions and biomass burning emissions predominate, and use ecoregions as a specific framework for understanding geographic variation in seasonality of trace N gas VCDs specifically and of the N cycle more generally.

2. Data and Methods

2.1. Satellite Products and Gridded Data Sets

We used observations of atmospheric NH_3 and carbon monoxide (CO) from the Infrared Atmospheric Sounding Interferometer (IASI), aboard the European Space Agency's Metop-A launched in 2006. IASI-A is a sun-synchronous polar-orbiting instrument with a spatial resolution of 12 km and swath width of about 2,200 km, resulting in near daily global coverage both during ascending and descending node. Here we use morning observations (9:30 local solar time equator crossing, descending node), when the thermal contrast is more favorable for retrievals (Clarisse et al., 2009; Van Damme et al., 2014). The NH_3 retrieval product used (ANNI-NNv2.2R-I, Van Damme et al., 2017) follows an earlier approach in which total columns of NH_3 are obtained by calculating a dimensionless spectral index (HRI), which is then converted into a NH_3 total column through the use of a neural network (Whitburn et al., 2016). The neural network uses a range of variables such as temperature and water vapor profiles to represent the state of the atmosphere as best as possible to produce the matching NH_3 total column for that atmospheric state. Only retrievals with cloud cover under 10% were used. For CO we used the product obtained with the FORLI v20140922 retrieval algorithm (Hurtmans et al., 2012), using retrievals with cloud cover under 25% and gridded to $0.5° \times 5°$ monthly resolution. Given the absence of hourly or even daily observations of NH_3 concentrations in sub-Saharan Africa, the detection limit of IASI is difficult to determine with certainty. However, the region experiences high thermal contrast, and IASI seems to be able to reliably observe down to 1–2 ppb at the surface (Van Damme et al., 2014).

We regridded the Level-2 IASI NH_3 product to a $0.25° \times 0.25°$ monthly resolution grid to match the resolution of other data used in the analysis. Specifically, we overlaid a subscale grid with a resolution of $0.02° \times 0.03°$ centered over each IASI observation, and extending over the entire elliptical satellite footprint. We added the observation value of the footprint for subscale gridcells within the IASI footprint to its corresponding 0.25° gridcell, weighted by the number of subscale observations included in the larger gridcell. Only subscale grid cells that are entirely within an IASI footprint are assigned an observation value, and only subscale grid cells that are entirely within a 0.25° gridcell are used to calculate its value. This approach was used so that grid cell values would more accurately reflect the observations within that grid cell, as opposed to, for example, assigning the entire observation footprint to the grid cell in which the footprint center is located. Each ecoregion included a minimum of at least 3,000 observations per month.

The IASI product has been validated using ground-based Fourier transform infrared (FTIR) observations of NH_3 total columns, with robust correlations at sites with high NH_3 concentrations, but lower at sites where atmospheric concentrations approach both instruments' detection limits (Dammers et al., 2017). Compared to the FTIR observations, total columns from previous IASI NH_3 products (Van Damme et al., 2014; Whitburn et al., 2016) are biased low by ~30% which varies per region depending on the local concentrations. The IASI NH_3 product was used for the years 2008—the first full year of data available—to the end of 2017. Because of the short lifetime of NH_3, most atmospheric NH_3 is assumed to be in the boundary layer (Dammers et al., 2019).

We also used the publicly available level 3 tropospheric NO_2 version 3 product from OMI, a nadir-viewing spectrometer measuring solar backscatter in the UV-visible range aboard NASA's Aura satellite (Krotkov et al., 2017). OMI is a sun-synchronous polar-orbiting instrument (13:45 local solar time equator crossing, ascending node) with a spatial resolution of 12 km and swath width of about 2,600 km, resulting in daily global coverage. The version 3 product uses a multi-step, iterative spectral fitting approach to retrieve slant column densities. The level 3 product is cloud-screened, including only grid cells that are at least 70% cloud-free, and provided at 0.25° resolution. Each ecoregion included a minimum of 12,000 observations per month; differences in retrieval algorithms and the less restrictive cloud screening contributed to greater coverage for NO_2 than NH_3 VCDs (see SI information; Tables S1–S4). The OMI product relies on air mass factors to calculate tropospheric VCDs from total slant column densities. The air mass factor is calculated with the assistance of an atmospheric chemical transport model, and is sensitive to model representations of emission, chemistry and transport data. These data are generally poorly constrained for regions not commonly analyzed in chemical transport models such as sub-Saharan Africa (McLinden et al., 2014). Additional bias may be introduced due to the reliance on nearly cloud-free grid cells, where greater sunlight may induce higher photochemical rates. For example, the current product is biased roughly 30% low over the Canadian oil sands (McLinden et al., 2014). The level 2 OMI-NO_2 product has been validated against in situ and surface-based observations in North America, Asia, and Europe, showing good agreement (Celarier et al., 2008; Krotkov et al., 2017; Lamsal et al., 2014). OMI data were used for the period 2005–2017, except in the statistical analysis of NO_2 and NH_3, when data from 2008 to 2017 were used.

Although IASI and OMI differ in observation time, the only analyses that include observations from both instruments are those considering CO and NO_2 VCDs. Because of the relatively long lifetime of CO, we do not expect our analyses to be sensitive to these differences.

The Tropical Rainfall Measuring Mission (TRMM) daily precipitation product (3B42) is based on a combination of TRMM observations, geo-synchronous infrared observations, and rain gauge observations (Huffman et al., 2007). Independent rain gauge observations from West Africa have been used to validate the product, with no indication of bias in the product (Nicholson et al., 2003).

We used the 500-m MCD64A1 collection 6 Moderate Resolution Imaging Spectroradiometer (MODIS) 500 m daily (Giglio et al., 2018). The burned area data are aggregated by month and gridded to 0.25° resolution.

GFED4s (van der Werf et al., 2017) provides monthly fire emissions at 0.25° resolution based on satellite-derived burned area (Giglio et al., 2013; Randerson et al., 2012) and a modified version of the Carnegie-Ames-Stanford-Approach biogeochemical model (Potter et al., 1993). Uncertainty in GFED4s fire emissions stems from uncertainty in burned area, fuel consumption, and emission factors, but is poorly constrained. According to van der Werf et al. (2017), a 1σ of about 50% for fire carbon emissions is a best-guess estimate for regional scale uncertainty assessment. This may also be a best-guess estimate for fire NH_3 and NOx emissions in our study region; although the uncertainty in NH_3 emissions maybe somewhat larger due to the small sample size of emissions factors (Akagi et al., 2011; van der Werf et al., 2017), and the uncertainty in NOx emissions is expected to be higher in regions where small fires make an important contribution to emissions (van der Werf et al., 2017). In general, burned area and fuel consumption in savannas are better constrained than in other biomes (Giglio et al., 2013; van der Werf et al., 2017).

We used the NOAA National Climatic Data Center's 0.5° gridded 2-m monthly land surface temperature product (Fan & van den Dool, 2008). The data set is based on a combination of station observations from the Global Historical Climatology Network version 2 and the Climate Anomaly Monitoring System (GHCN_CAMS) and uses an anomaly interpolation approach which relies on observation-based reanalysis data to derive spatio-temporal variation in temperature lapse rates for topographic temperature adjustment.

2.2. Ecoregions

We used The Nature Conservancy's (TNC) map of Terrestrial Ecosystems (available at http://maps.tnc.org/gis_data.html), an updated version of Olson and Dinerstein (2002), as the basis for our ecoregion-based analyses (Figure 1). In order to conduct a broad regional analysis, we created five of our ecoregions by combining two or more ecoregions as defined in the TNC map: our wet savanna ecoregion was created by combining East Sudanian Savanna, West Sudanian Savanna, and Saharan Flooded Grasslands; our Northern

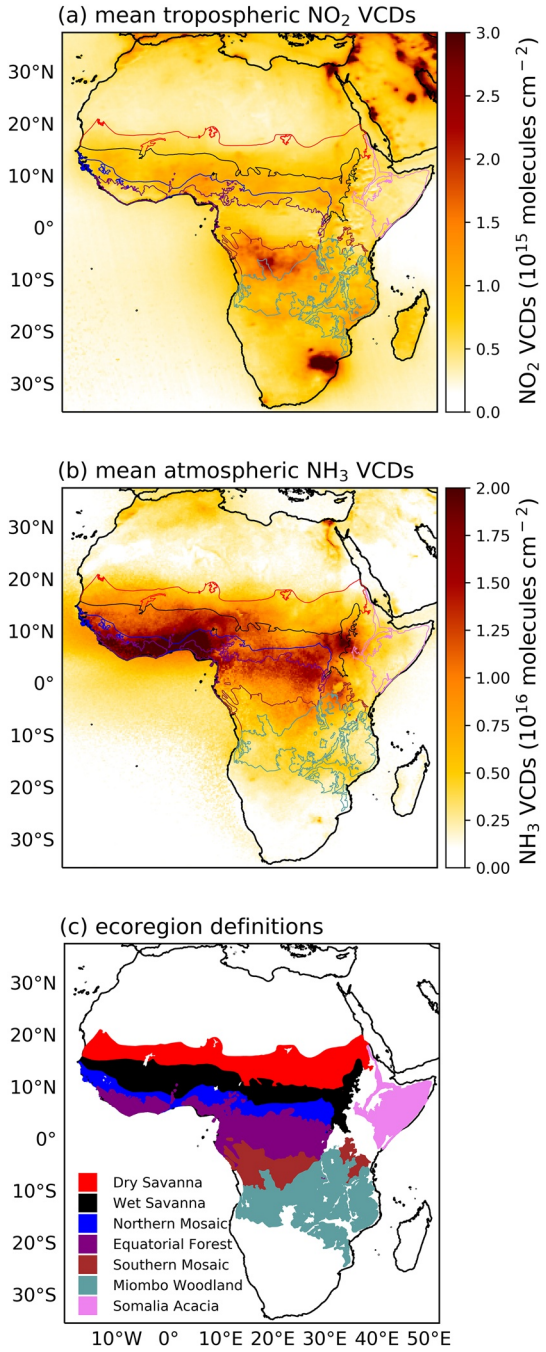

Figure 1. Mean annual nitrogen dioxide (NO_2) and ammonia (NH_3) vertical column densities (VCDs) and ecoregion definitions. (a) Long-term mean tropospheric NO_2 VCDs as observed by Ozone Monitoring Instrument (2005–2017). (b) Long-term mean atmospheric NH_3 VCDs as observed by Infrared Atmospheric Sounding Interferometer (2008–2017). (c) Boundaries of seven major African ecoregions evaluated in this study. Long-term mean VCD values are calculated from the monthly means.

Mosaic ecoregion consists of Guinean and North Congolian Forest-Savanna mosaics; our equatorial forest ecoregion was formed by combining multiple Congolian Forest ecoregions with Equatorial Coastal, Nigerian, Guinean, and Cameroonian Forest ecoregions; our Southern Mosaic region consists of Southern and Western Congolian forest-savanna mosaic along with Southern Acacia-Commiphora bushlands and thickets; our Miombo ecoregion consists of Eastern, Western, Central Zambizian, and Angolan Miombo woodlands. In addition, we simplified some of the masks to exclude small gaps in ecoregion cover or isolated small additional areas of ecoregion cover outside of the main mask area, or where there were isolated ecoregion patches at a distinct latitude from the main ecoregion area. The shapefiles used to create the masks are archived as a supplementary file.

2.3. Statistical Analyses

First, we explored the relationship between seasonal precipitation patterns and VCDs of NO_2 and NH_3 by (a) calculating the per 0.25° grid cell Pearson's product moment correlation coefficient based on monthly time series, and (b) analyzing how these patterns vary across gradients of MAP. Second, to explore other potential drivers of seasonal variability, we repeat this analysis for relationships between trace gas VCDs and burned area, CO, and temperature. In analyses involving the GHCN_CAMS surface temperature data set, other data were regridded to 0.5° resolution prior to analyses by taking the mean of all 0.25° grid cells within each larger 0.5° grid cell. Analyses were conducted using Python v3.6.3.

Third, we developed ecoregion-scale statistical models to explore drivers of seasonal variation in NH_3 and NO_2 VCDs, using temperature, precipitation, burned area, and CO VCDs as predictor variables for the period 2008 through 2017. For each ecoregion, we first calculated monthly time series of each variable based on the mean of all grid cells located within the ecoregion mask. Because the seasonal cycle is typically at least two orders of magnitude larger than observed decadal trends, we did not remove long-term trends; summaries of the number of satellite observations used for each monthly mean and associated errors are presented in the supplemental information (Text S1; Tables S1–S4). Based on the monthly data, we used multiple linear regression to understand the relative importance of each explanatory variable for seasonal variation in NH_3 and NO_2 VCDs separately. In addition to the full-year analyses, we conducted separate analyses for either the rainy or dry season months, since the relationships between some variables can change in direction depending on the season, and because we expect different sources to be important depending on the season. We used a threshold of 20 mm precipitation $month^{-1}$ to classify each month for each year as occurring during the dry or rainy season (Kniveton et al., 2009), resulting in a clear separation between wet and dry season for all ecoregions except Equatorial forest. Where analyses met the assumptions of linear regression, we conducted multiple linear regression, transforming data as necessary, using log, square root, arcsin, or rank transformation, and excluding single outliers as needed. In some analyses, one or two predictor variables were removed to address multicollinearity when variance inflation factors exceeded 5; the transformations used in each analysis are detailed in the supplemental information (Table S5). When the assumptions of homogeneity of variances and normality could not be met—which was only the case in analyses involving NO_2

VCDs—we used a generalized linear model instead of multiple linear regression. Analyses were conducted using R v.3.5.0

In all analyses and figure panels incorporating multiple data sets with historical records of different lengths, the analysis uses only historical periods covered by all data sets. So, for example, analyses including IASI NH_3 VCDs and TRMM observations use observations for 2008 through 2017, whereas analyses including OMI tropospheric NO_2 VCDs and TRMM observations use observations from 2005 through 2017.

3. Results and Discussion

3.1. MAP Controls Geographic Distribution of NO_2 and NH_3 Emission Sources and Seasonality

Annual rainfall appears to determine how different seasonal patterns of emissions are distributed geographically across the African continent, and at least for NO_2, where soil versus biomass burning sources are important determinants of seasonal variation in VCDs. A critical threshold can be observed at roughly 500 mm precipitation yr^{-1}, separating Africa into regions with low and high MAP that have distinct relationships between monthly precipitation and monthly NO_2 and NH_3 VCDs (Figure 2). Figure 3 illustrates these thresholds and relationships by examining how the direction and strength of the correlation between monthly precipitation and mean monthly atmospheric VCDs of NO_2 and NH_3 changes at different levels of MAP. At MAP levels below 500 mm yr^{-1}, months with higher precipitation are associated with higher VCDs of both gases—that is, VCDs tend to be highest during the rainy season—implying that soil emissions are a critical driver of seasonality in trace gas VCDs in these ecoregions.

When MAP ranges from roughly 500–1,750 mm yr^{-1}, that relationship reverses, so that months with higher precipitation result in lower VCDs of both gases—VCDs tend to be highest during the dry season of these more mesic ecoregions. The change in sign for the monthly precipitation-NO_2 relationship (and potentially of the precipitation-NH_3 relationship) from positive below 500 mm yr^{-1} to negative above it can be attributed to a shift from seasonal changes in soil emissions driving trace gas VCD seasonality in dry regions to variation in biomass burning emissions driving it in more mesic regions. The strong dependency of NO_2 seasonality on biomass burning in regions where MAP is between 500 and 1,750 mm yr^{-1} is further evident when mapping the correlation coefficients for the relationship between monthly NO_2 VCDs and monthly burned area with MAP isolines (Figure S1).

Geographically, MAP is an important determinant of ecosystem type, and the 500 mm and 1,500–1,750 mm thresholds we identified correspond well to ecoregion boundaries (Figure S2). The 500 mm yr^{-1} threshold broadly corresponds to a shift from the Somalia Acacia ecoregions to more mesic ecoregions in the east, and from dry savanna to wet savanna in the north. As expected, these ecoregion transitions are generally also accompanied by a marked increase in annual burned area (Figure S3). The 1,500–1,750 mm yr^{-1} threshold generally corresponds to the transition to equatorial forest, a marked decline in burned area, and a reduction in precipitation seasonality. These geographic patterns suggest that MAP influences the relationship between monthly precipitation and trace gas VCDs in part by determining the distributions of different types of vegetation cover.

These results extend earlier site-based analyses comparing sites in north equatorial dry savanna, wet savanna, and equatorial forest (Adon et al., 2010; Ossohou et al., 2019). In these site-based studies, soils were found to drive seasonality of NO_2 in the northern dry savanna sites, where MAP was less than ~800 mm yr^{-1}, though concentrations at one site were also influenced by biomass burning emissions (Adon et al., 2010; Delon et al., 2010; Ossohou et al., 2019). NO_2 concentrations were low during the dry season at these sites and high during the rainy season, suggesting a positive relationship between monthly precipitation and NO_2 concentrations. In contrast, in sites studied in lower latitudes where MAP was above ~1,200 mm yr^{-1}, biomass burning emissions emerged as the primary determinant of NO_2 seasonality, leading to elevated concentrations during the dry season (Ossohou et al., 2019). Similar patterns were also found for NH_3—in sites with MAP less than ~800, concentrations were elevated during the rainy season and attributed to soil emissions, whereas in sites MAP higher than ~1,200 mm yr^{-1}, concentrations were elevated during the dry season, and attributed to biomass burning (Adon et al., 2010)—which are also consistent with our regional analysis (e.g., Figures 2 and 3). To our knowledge, these patterns have not been evaluated at regional scales.

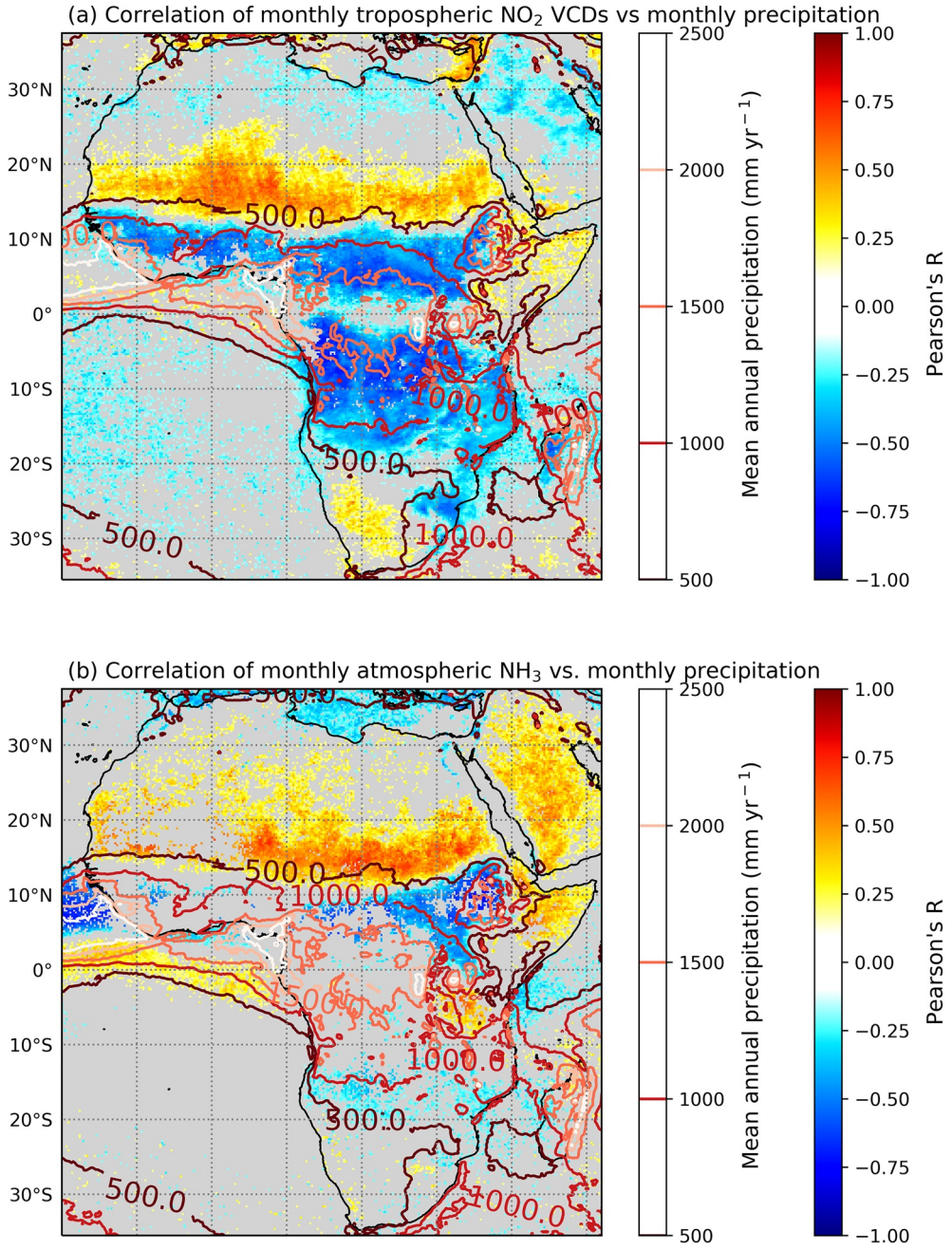

Figure 2. Relationship between monthly precipitation and monthly nitrogen dioxide (NO_2) (2005–2017) or ammonia (NH_3) vertical column densities (VCDs) (2008–2017). Per grid cell correlation coefficients between mean monthly precipitation and (a) tropospheric NO_2 VCDs and (b) atmospheric NH_3 VCDs overlaid with mean annual precipitation isolines. Gray areas indicate region with insignificant correlation ($p > 0.05$).

A notable exception to the overall pattern occurs in Tanzania, where the relationship between monthly precipitation and NH_3 VCDs is positive even though MAP is above 500 mm yr^{-1} (Figure 2b). Part of this positive relationship is over the area in Tanzania and Kenya where 1.5 million wildebeest migrate, following the movement of the ITCZ (Serneels & Lambin, 2001). There is tight coupling between animal migration and monthly precipitation in this region; it is possible that this migration may contribute to the positive relationship between monthly precipitation and NH_3 VCDs observed here. We note more broadly that excreta from wild animals could be a regionally important source of NH_3, though it is challenging to evaluate

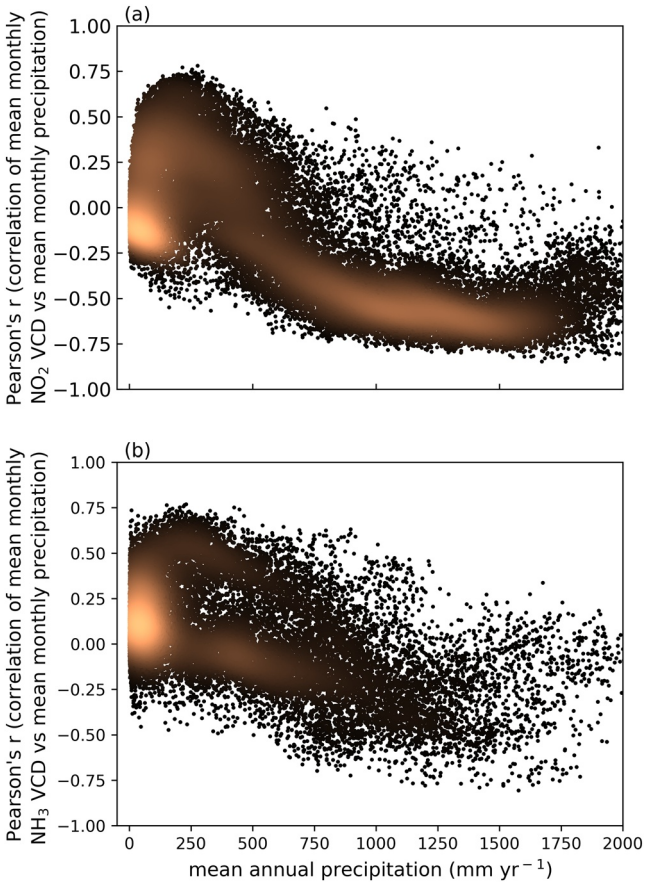

Figure 3. Mean annual precipitation (MAP, mm yr^{-1}) determines the direction and strength of the correlation between mean monthly precipitation and (a) mean monthly tropospheric nitrogen dioxide (NO_2) vertical column density (VCD) (2005–2017) and (b) mean monthly atmospheric ammonia (NH_3) VCD (2008–2017) for 0.25° grid cells over all of continental Africa. Precipitation values are from Tropical Rainfall Measuring Mission, and NO_2 and NH_3 data are from Ozone Monitoring Instrument and Infrared Atmospheric Sounding Interferometer, respectively. Lighter shades of copper represent a higher density of grid cells.

at regional scales given the lack of spatially explicit data sets. However, early estimates suggest that emissions from wild animals represent less than 1% of NH_3 emissions from Africa (Bouwman et al., 1997).

3.2. Seasonal Variation in NO_2 and NH_3 VCDs Across African Ecoregions

Atmospheric VCDs of both NO_2 and NH_3 exhibit clear seasonal patterns that vary distinctly by ecoregion (Figures 4 and 5, Table 1; note that scales for VCDs and biomass burning emissions vary between Figures 4 and 5). Overall, the peak monthly NH_3 VCDs exceed those of tropospheric NO_2 for most ecoregions (Figures 4 and 5), as do mean annual concentrations (Figure 1). In the dry ecoregions of dry savanna and Somalia Acacia, VCDs of NO_2 and NH_3 tend to be higher in the rainy season than in the dry season. In more mesic ecoregions—with the exception of equatorial forest, which lacks a distinct dry and rainy season—the pattern is reversed: NO_2 and NH_3 VCDs tend to decrease during the rainy season, and to increase during the dry season. As discussed in Section 3.1, this overall pattern is what would be expected if dry and mesic ecoregions have distinctly different seasonal regimes of trace N gas emissions, related to differences in the relative importance and seasonality of soil and biomass burning emissions.

As noted in Section 1, fossil fuel emissions of NO_2 in sub-Saharan Africa are low relative to seasonal sources of NO_x such as biomass burning and nitrification in soils (Jaeglé et al., 2005). For example, across 80% of the mesic savannas in Africa, fossil fuel emissions are estimated to be equivalent to roughly 2% of dry season emissions from biomass burning (Hoesly et al., 2017; van der Werf et al., 2006), and analysis of data from OMI suggests that that estimate is likely a substantial overestimate (Hickman et al., 2021). In addition, on the basis of emissions inventories and previous analyses of satellite observations, we do not expect strong seasonal variations of fossil fuel NO_x emissions (Hoesly et al., 2017; van der A et al., 2008). Lightning is also a source of atmospheric NO_x, though it makes a small contribution to African NO_x emissions (Jaeglé et al., 2005) or their seasonality (Figure S4).

To further evaluate the importance of soil and biomass burning emissions for the seasonality of NO_2 and NH_3 VCDs over sub-Saharan Africa, we conduct statistical analyses to evaluate four variables that are likely to be related to seasonal variation in those emission sources: precipitation, temperature, burned area, and CO VCDs. Because the nature of the covariance between these variables can change depending on whether rainy or dry season months are considered (Figure S5), we evaluate relationships first using the entire data set, and then considering data for the rainy and dry seasons separately. We included CO VCDs as an indicator of biomass burning emissions in addition to burned area estimates because coarse resolution global burned area products strongly underestimate fire activity outside the peak burning months (Ramo et al., 2021; Roteta et al., 2019), which is when emission factors may shift from the emission of more oxidized to less oxidized species, like NH_3 (Zheng et al., 2018). It should be noted that at 1–2 months, the lifetime of CO is considerably longer than that of NH_3, resulting in considerable transport across the study region. CO VCDs have been used as an indicator of smoldering biomass burning emissions (Zheng et al., 2018), and the co-emission of the two species from smoldering fires has made it a useful indicator for biomass burning emissions of NH_3 (Whitburn et al., 2015). CO VCDs are often correlated with aerosol optical density (AOD) over biomass burning regions (Edwards et al., 2006), and can be a better tracer for emissions than AOD in regions where dust sources are large, such as north equatorial sub-Saharan Africa. Indeed, monthly values of AOD tend to exhibit similar seasonality to CO VCDs over African ecoregions (Figures S4 and S6).

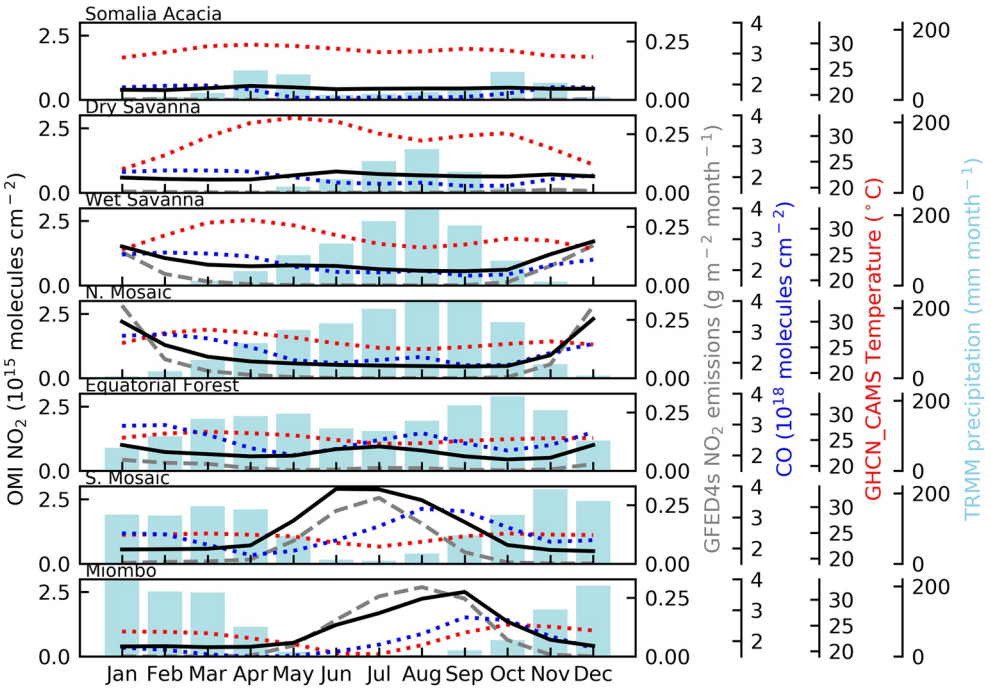

Figure 4. Seasonal variability in nitrogen dioxide (NO_2) vertical column densities (VCDs) and related variables or drivers for seven major ecoregions in sub-Saharan Africa, 2005–2017. Total monthly precipitation (blue bars, mm month^{-1}) and mean monthly surface temperature (dotted red line, °C), tropospheric NO_2 VCDs (solid black line, 10^{15} molecules cm^{-2}), atmospheric carbon monoxide (CO) VCDs (dotted blue line, 10^{18} molecules cm^{-2}), and biomass burning emissions of NO_2 (dashed gray line, g m^{-2} month^{-1}) are presented. GHCN_CAMS, Global Historical Climatology Network version 2 and the Climate Anomaly Monitoring System; OMI, Ozone Monitoring Instrument; TRMM, Tropical Rainfall Measuring Mission.

3.2.1. NO_2 Seasonality

In examining the effects of monthly burned area and precipitation on NO_2 seasonality, we find two general control regimes, reflecting the continental-scale patterns observed in Section 3.1: generally, biomass burning appears to be the primary driver of NO_2 seasonality over the more mesic ecoregions, whereas biogenic sources appear to be more important in the two dry ecoregions.

In mesic ecoregions with distinct rainy and dry seasons, there was a close temporal correspondence between NO_2 VCDs and biomass burning emission of NO_2 from GFED4s (Figure 4), and monthly burned area explained most of the variation in monthly NO_2 VCDs (Figure 4, Table 2). Monthly precipitation—which would tend to suppress biomass burning, suppress emissions of more oxidized compounds (including NO) when biomass burning occurs, and increase wet deposition of HNO_3 and other species—was always negatively related to NO_2 VCDs (Figure 4, Table 2). As expected for these ecoregions, these results support a central role for biomass burning in determining the seasonality of NO_2 VCDs. These patterns also hold when analyzing dry and rainy seasons separately: monthly burned area and CO VCDs were the only significant predictors of monthly NO_2 VCDs during the dry season across the mesic ecoregions (Table S6). A significant positive relationship between NO_2 and biomass burning was also found for three of the mesic ecoregions during the rainy season, likely reflecting greater burning emissions during shoulder rainy season months with relatively low precipitation than during the mid-rainy season.

The importance of biomass burning as a source of NO_x in African savannas and woodland is well known, representing over half of all biomass burning emissions of NO_x globally (Jaeglé et al., 2005; van der Werf et al., 2017). Its central role in seasonality of NO_2 concentrations in biomass burning regions has been documented in emission inventories and studies using satellite observations (Hickman et al., 2021; Mebust & Cohen, 2013; van der Werf et al., 2017; Whitburn et al., 2015), but it is only in site-level studies that its role in the seasonality of NO_2 concentrations in specific African ecoregions—dry savanna, wet savanna,

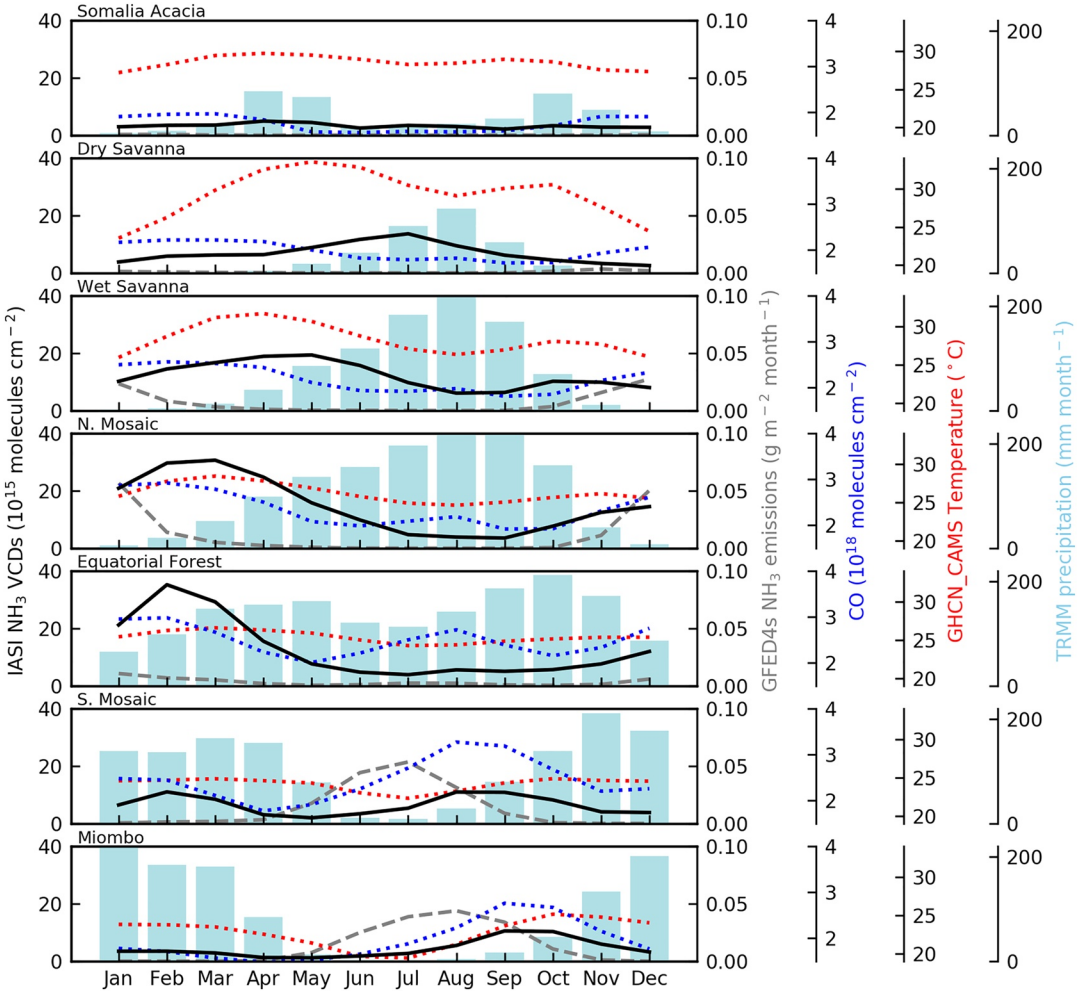

Figure 5. Seasonal variability in ammonia (NH_3) vertical column densities (VCDs) and related variables or drivers for seven major ecoregions in sub-Saharan Africa, 2008–2017. Total monthly precipitation (blue bars, mm month^{-1}), mean monthly surface temperature (dotted red line, °C), atmospheric NH_3 VCDs (solid black line, 10^{15} molecules cm^{-2}), atmospheric carbon monoxide (CO) VCDs (dotted blue line, 10^{18} molecules cm^{-2}), and biomass burning emissions of NH_3 (dashed gray line, g m^{-2} month^{-1}) are presented. GHCN_CAMS, Global Historical Climatology Network version 2 and the Climate Anomaly Monitoring System; IASI, Infrared Atmospheric Sounding Interferometer; TRMM, Tropical Rainfall Measuring Mission.

Table 1
Mean Atmospheric NH_3 (2008–2017) and Tropospheric NO_2 VCDs (2005–2017) for Each Ecoregion During the Dry and Rainy Seasons in Units of 1×10^{13} Molecules cm^{-2}

	Dry savanna	Wet savanna	Northern Mosaic	Equatorial forest	Southern Mosaic	Miombo woodland	Somalia Acacia
Dry season NH_3	488 (25)	1,187 (54)	1,998 (130)		517 (63)	407 (50)	286 (14)
Rainy season NH_3	1,013 (47)	1,232 (67)	1,333 (105)	1,282 (99)	681 (40)	460 (36)	366 (18)
Dry season NO_2	58.6 (0.9)	126.3 (4.4)	198.3 (8.4)		286.9 (3.2)	164.9 (8.9)	41.2 (0.4)
Rainy season NO_2	69.7 (1.0)	65.7 (1.1)	60.5 (1.8)	72 (2)	97.4 (5.6)	61.4 (4.7)	46.3 (0.6)

Notes. Means were calculated from monthly mean VCDs, and the rainy and dry seasons were defined as months when the mean precipitation for the ecoregion was greater than or less than 20 mm rainfall month^{-1}, respectively. Ecoregions are defined as indicated in Figure 1. The standard error of the mean is presented in parentheses, but does not consider within-ecoregion variability, and so should be considered as a lower estimate.
Abbreviations: NH_3, ammonia; NO_2, nitrogen dioxide; VCDs, vertical column densities.

Table 2
The Relationship Between Monthly Mean Temperature, Rainfall, or Burned Area and VCDs of Atmospheric NH_3 or Tropospheric NO_2 Across Seven Ecoregions in Sub-Saharan Africa

	Somalia Acacia	Dry savanna	Wet savanna	Northern Mosaic	Equatorial forest	Southern Mosaic	Miombo woodland
	NH_3						
Total model	0.21***	0.72***	0.75***	0.90***	0.75***	0.50***	0.82***
Temperature	n.s.	0.29***	0.71***	0.71***	0.67***	n.s.	0.10***
Precipitation	0.12***	0.25***	n.s.	0.28***	n.s.	0.09**	n.s.
Burned area	n.s.	0.10***			0.09**	0.16***	
CO VCDs	n.s.	0.06*	n.s.	0.16***	0.08**	0.28***	0.57***
	NO_2						
Total model	0.45***	0.35***	0.88***	0.94***	0.73***	*0.95****	*0.97****
Temperature	0.15***	n.s.			0.24***	*0.12****	*0.05****
Precipitation	0.26***	0.05*	0.09***	0.44***	0.51***	*0.15****	*0.05****
Burned area	n.s.	0.05*	0.71***	0.77***	n.s.	*0.65****	*0.81****
CO VCDs	n.s.	0.10***	0.07**	0.12***	n.s.	*0.32****	*0.16****

*** $p<0.001$ ** $p<0.01$ * $p<0.05$ n.s.: not significant

Coefficients of partial determination:

<0.1	*<0.1*
0.1 to 0.5	*0.1 to 0.5*
>0.5	*>0.5*

Notes. R^2 values are listed for the full model, and coefficients of partial determination are listed for each predictor variable. Blue shades represent positive relationships and red shades represent negative relationships. Dark gray cells indicate variables that were not included in the model to avoid issues of multicollinearity. Results in italics were calculated using generalized linear models in cases where the assumptions of linear regression could not be met. Analyses used data spanning from 2008 through 2017. Separate results for the wet and dry season-only models are shown in Table S6.

Abbreviations: CO, carbon monoxide; NH_3, ammonia; NO_2, nitrogen dioxide; VCDs, vertical column densities.

and forest—has been investigated (Adon et al., 2010; Delon et al., 2010; Martins et al., 2007; Ossohou et al., 2019). Our results are broadly consistent with these earlier studies, though where we did not find an overall relationship between monthly burned area and monthly NO_2 in the dry savanna, one of the INDAAF dry savanna sites found that biomass burning contributed to NO_2 seasonality (Adon et al., 2010; Delon et al., 2010). These results likely differ from ours for two reasons: first, the site—Katibougou, Mali—is subject to biofuel emissions as well as biomass burning (Delon et al., 2010), and second, it is located in the northern part of the wet savanna as defined in our study, rather than in our dry savanna ecoregion (Olson & Dinerstein, 2002). We also note that we did find a relationship between monthly burned area and monthly NO_2 in the dry savanna when considering only the dry season, suggesting that within the low-emission context of the dry season, local biomass burning emissions can be non-negligible contributors to local seasonal dynamics in dry savannas.

We do also find significant positive relationships between temperature and NO_2 VCDs in the Miombo (Table 2). Although temperature explains only a tiny portion of the annual variation in NO_2 VCDs, it is more important during the rainy season (Table S6), suggesting a role for biogenic emissions in determining sub-seasonal variation in NO_2 VCDs. We are unaware of other studies that have investigated this relation-

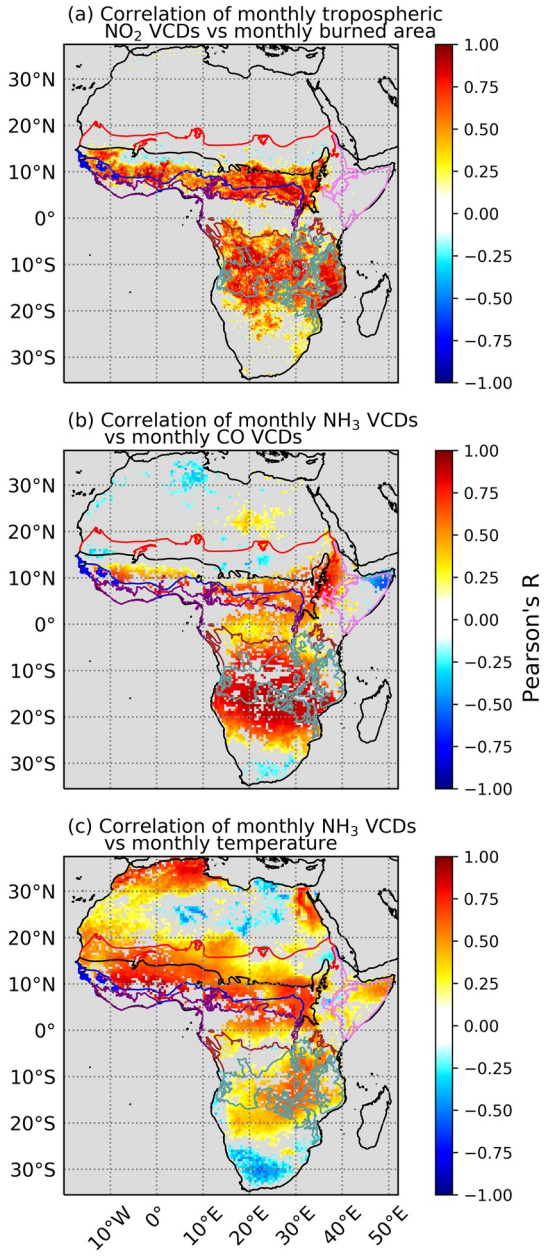

Figure 6. Map of correlation coefficients for the relationship between (a) mean monthly tropospheric nitrogen dioxide (NO_2) vertical column densities (VCDs) and burned area (2005–2017), (b) mean monthly atmospheric ammonia (NH_3) and carbon monoxide (CO) VCDs (2008–2017), and (c) mean monthly atmospheric NH_3 VCDs and land surface temperature (2008–2017) overlaid with ecoregion boundaries. Values are included only over land where the relationship is significant at $p < 0.05$. Additional analyses for NH_3 VCDs and burned area, NO_2 and CO VCDs, and NO_2 and NH_3 VCDs and AOD are included as Figures S1b, S4, and S6–S8.

ship in the Miombo woodland, though rainy season soil emissions have been suggested to be a substantial NO_2 source in tropical rainforest (Adon et al., 2010), which suggests a possible role for temperature.

In contrast to the mesic ecoregions, precipitation and temperature were positively related to NO_2 VCDs in the two dry ecoregions (Figure 4, Table 2), consistent with variation in soil microbial activity being a critical driver of seasonality in NO_2 VCDs. The relationship with precipitation is also significant when considering rainy and dry seasons separately (Table S6). Precipitation has long been shown to be an important control over biogenic N cycling and NO emissions (Davidson, 1992; Davidson et al., 1993), including in sub-Saharan Africa (Birch, 1960; Dick et al., 2001; Jaeglé et al., 2004). It is likely that the Birch Effect—the increase in biogeochemical activity, nitrification, and enhanced emissions of NO that occurs when dry soils are wetted, particularly in seasonally dry ecosystems (Birch, 1958; Davidson et al., 1991; Delon et al., 2019)—is an important component of the precipitation effects on NO_2 seasonality. Earlier remote-sensing work has demonstrated that the Birch Effect results in substantial enhancement of tropospheric NO_2 concentrations over the Sahel during the early months of the rainy season (Hudman et al., 2012; Jaeglé et al., 2004), but also after smaller precipitation events at the end of the dry season (Hudman et al., 2012). The presence of a positive relationship between monthly temperature and NO_2 during the rainy season provides additional evidence pointing to the importance of biogenic soil NO emissions—which is also a temperature-dependent process—in determining the seasonality of NO_2 VCDs in dry ecoregions. In general, temperature has not been evaluated as a driver of NO emissions in African ecosystems outside of site-specific or laboratory studies, which tend to focus on short-term responses and diurnal variation (Feig et al., 2008; Meixner et al., 1997; Otter et al., 1999), though a multi-year study in a semi-arid South African savanna observed seasonal patterns in soil NO emissions that matched seasonal variation in soil temperature (Feig et al., 2008).

Site-scale studies in the dry savannas have found similar relationships with precipitation to our regional assessment, observing higher concentrations during the rainy season, as well as evidence of pulsed emissions during the first precipitation events, consistent with our interpretation of the importance of soil emissions to seasonal variation in NO_2 VCDs in dry ecoregions (Delon et al., 2010, 2019; Ossohou et al., 2019). Biomass burning emissions are relatively low in this ecoregion, estimated as roughly 1/5 to ½ of biomass burning emissions from more mesic African ecoregions (Galy-Lacaux & Delon, 2014). Still, burned area was significantly related to monthly NO_2 VCDs during the dry savanna dry season, which may partly reflect the influence of biomass burning in east and south of this ecoregion, where MAP exceeds 500 mm yr^{-1}.

The equatorial forest ecoregion differs from other mesic ecoregions in that it lacks a distinct dry season, and less biomass burning occurs there; nevertheless, biomass burning appears to be an important influence on NO_2 seasonality. In this region, NO_2 VCDs have a somewhat bimodal distribution that includes a second peak mid-year (Figure 4). The bimodal NO_2 seasonality is likely driven by biomass burning in the northern and southern parts of the equatorial forest ecoregion: the timing of the bimodal peaks corresponds in time to the peaks in adjacent ecoregions to the north and south that are related to biomass burning (Figure 6a), and generally corresponds to seasonal

variation in biomass burning emissions of NO_2 from GFED4s (Figure 5). This interpretation is also consistent with the strong negative relationship between monthly precipitation and NO_2 VCDs (Table 2, Table S6).

Earlier, site-scale work observed somewhat different seasonal patterns in equatorial forest. A field study in the Mayombe equatorial rainforest of Congo observed soil NO emissions that were three times larger in the wet season than the dry season, though much of the emitted NO_x is expected to be intercepted by the plant canopy (Adon et al., 2010; Serça et al., 1998). Long-term measurements at forest sites in Cameroon and Congo found that NO_2 concentrations were roughly comparable in the sites' wet (March through November) and dry seasons (December through January), and researchers inferred that biomass burning and soil emissions after canopy interception were similar in magnitude (Adon et al., 2010). However, sampling at these sites was conducted at 1.5–3 m above the ground, and so appears unlikely to capture the full effect of canopy interception. Upper canopy interception may reduce transport of emitted soil NO_x above the forest canopy, which could explain the patterns we observe from space suggestive of a larger influence of biomass burning emissions on seasonality of tropospheric NO_2 VCDs.

Although the patterns that we observe are consistent with emissions being responsible for seasonal variation in NO_2, it is possible that changes in NO_x chemistry could influence its lifetime and affect seasonal variation. However, numerical model analyses suggest that changes in chemistry are driven primarily by the effect of emissions on atmospheric NO_x burden. Because higher NO_x burdens drive increased net NO_x chemistry, changes in net chemistry would generally be in the opposite direction of changes in emissions or atmospheric concentrations (see supplementary materials; Figure S9). Lastly, we note that we do not find strong evidence that these patterns hold over interannual timescales, but that may be the result of the relatively short satellite record, which reduces the statistical power for these analyses (Table S7).

3.2.2. NH_3 Seasonality

Broadly similar to what we observed for NO_2 seasonality, we find that variation in emissions from soil and livestock excreta are likely the critical control over the seasonality of NH_3 VCDs in dry ecoregions. But in mesic ecoregions, seasonal variation in a combination of sources appears to be responsible for the NH_3 seasonality, and the relative importance of different drivers varies between the northern and southern hemisphere. As with NO_2, statistical power may limit our ability to observe similar patterns over interannual timescales (Table S7).

Temperature exerts a uniformly positive control over NH_3 variability in ecoregions where the relationship is significant, whether considering the entire year or rainy and dry seasons individually (Table 2, Table S6, Figure 6c). Because NH_3 volatilization is a temperature-dependent process (Sutton et al., 2013), these positive relationships suggest that volatilization of NH_3 from soil and animal excreta contributes to seasonality in NH_3 VCDs in both mesic and dry ecoregions. In the two dry ecoregions, monthly precipitation is also positively related to NH_3 VCDs, whereas burned area is not (Table 2, Table S6), which together with a significant role for temperature suggest that soil and animal excreta emissions are the primary control over NH_3 seasonality in these environments. This positive relationship between precipitation, temperature, and NH_3 VCDs is consistent with observations from a network of passive sampling sites in the dry savanna ecoregion, where NH_3 emissions, concentrations, and deposition were found to increase during the rainy season (Adon et al., 2010; Delon et al., 2012; Galy-Lacaux & Modi, 1998), and with analyses in a semi-arid ecosystem in Senegal, which also found positive relationships between NH_3 emissions and temperature during the rainy season (Delon et al., 2019). Livestock specifically has been identified as the main source of NH_3 emissions in the region (Delon et al., 2010), and is characterized by higher emissions during the wet season (Delon et al., 2012). Seasonality in NH_3 emissions is likely the result of changes in temperature and precipitation, as well as changes in excreta quantity and quality, which peak in the late rainy season because animals tend to be better fed (Schlecht & Hiernaux, 2004; Schlecht et al., 2006).

Precipitation can increase NH_3 emissions by increasing soil moisture, which tends to increase volatilization of soil NH_3 (Al-Kanani et al., 1991; Sommer et al., 2004), as well as enhance soil nitrogen mineralization and urease activity, which provides additional substrate for NH_3 volatilization (Birch, 1958; Placella et al., 2012; Sahrawat, 1984). Precipitation events have also been shown to induce large pulses of NH_3 emissions over the Sahel (Hickman et al., 2018), as well as in other dryland sites (Soper et al., 2016). It can also enhance wet deposition: in the Senegalese semi-arid ecosystem, high rainfall in August effectively leaches atmospheric

NH_3, leading to a decrease from the July peak in NH_3, similar to the pattern we observe for the dry savanna ecoregion (Delon et al., 2019). In addition, NH_3 VCDs have been found to increase substantially following the receding of the water extent of Lake Natron in Tanzania (Clarisse et al., 2019) and of wetland extent in the Sudd (Hickman et al., 2020), highlighting the importance of changes in soil moisture for soil emissions.

The dry savanna ecoregion does have a positive relationship between monthly CO and NH_3 VCDs in analyses of the full year and of the dry season (Table 2, Table S6), suggesting that biomass burning may also influence NH_3 seasonality there. As with the relationship between NO_2 VCDs and burned area, we expect these are related to the influence of seasonal variation in biomass burning in the south and east (Figure 6b). However, CO VCDs are a less important predictor than either precipitation or temperature in the dry savanna (Table 2).

Although increases in NH_3 VCDs tend to lag 1–2 months behind increases in burned area, GFED4s NH_3 emissions, and NO_2 VCDs (Figures 4 and 5), monthly CO VCDs—which are indicative of incomplete biomass combustion—are significantly and positively related to NH_3 VCDs in four of the mesic ecoregions (Table 2, Figure 6b). This relationship between CO and NH_3 VCDs suggests that like temperature, seasonal changes in biomass burning contribute to NH_3 seasonality across a number of ecoregions. Earlier work using IASI had also observed a lag between seasonal increases in NH_3 VCDs—which peaked in February in north equatorial Africa—and biomass burning as indicated by fire radiative power and CO VCDs (Whitburn et al., 2015), which can also be seen to some extent in our analysis of mesic ecoregions in the northern hemisphere. Whitburn et al. (2015) hypothesized that this lag could be related to elevated soil emissions following fire, though we did not find any spatial associations between previously burned area and NH_3 VCDs in February or March. It is possible that these late season NH_3 emissions are, instead, related to biomass burning, particularly from small fires. Recent analyses suggest that MODIS underestimates burned area during this period by a factor of roughly 2–5 because it is unable to detect many small fires (Ramo et al., 2021; Roteta et al., 2019). This is also the time of the year when more smoldering fires are expected, and when emission factors have been suggested to shift to favor less oxidized species (Zheng et al., 2018), possibly as a result of a shift to woodier fuel (van der Werf et al., 2006). Earlier work has observed a complementary shift in an analog for emission factors of NO_x, with a shift toward greater smoldering combustion (Mebust & Cohen, 2013), and long-term measurements from the INDAAF network concluded that NH_3 seasonality in the wet savanna and forest ecosystems is the result of biomass burning, with concentrations roughly doubling during the dry season (Adon et al., 2010).

The importance of both temperature and CO VCDs varies substantially among the mesic ecoregions, dividing ecoregions into those where temperature is the most important predictor of NH_3 seasonality, and those where CO VCDs are. In the three central and northern mesic ecoregions, temperature explains at least two thirds of the variation in NH_3 VCDs over the year, whereas CO VCDs explain less than one seventh. But in the Southern Mosaic and Miombo ecoregions CO VCDs are the most important of the environmental predictor evaluated, and temperature is either not significant or a relatively weak predictor (Table 2).

Livestock densities appear to be one important factor contributing to these differences between ecoregions in the northern and southern hemisphere. On average, livestock densities are two to four times higher in the northern biomass burning region than in the southern region: mean values are 9 and 17 Tropical Livestock Units (TLU) km^{-2} in the Northern Mosaic and wet savanna ecoregions, respectively, as compared to 5 and 4 TLU km^{-2} in the Southern Mosaic and Miombo ecoregions. The high livestock density ecoregions would be expected to be accompanied by similarly high excretion rates, and consequently more substrate for temperature-dependent NH_3 volatilization, which is consistent with the temperature-dependent patterns of NH_3 seasonality we observe in the northern hemisphere.

Differences in the kind of vegetation burned may also contribute to the different controls over seasonality in the northern and southern mesic ecoregions. As noted above, previous work has shown that peak NH_3 and CO VCDs lag 1–2 months behind peak fire radiative power in the southern biomass burning region (Whitburn et al., 2015), where CO VCDs tend to be highest over Miombo woodland areas (Zheng et al., 2018). This lag has been hypothesized to have been caused by a shift to more burning of woody biomass late in the fire season, causing increased emissions of less oxidized compounds such as CO and NH_3 (van der Werf

et al., 2006; Zheng et al., 2018). Woody biomass is widely burned in the southern biomass burning region (Sinha et al., 2004), but is less important in the northern region (Roberts et al., 2018).

NH_3 VCDs tend to begin their seasonal increase before the onset of the rainy season (Figure 5), suggesting that fertilizer applications—which typically occur after the start of the rainy season—may not be a major contributor to the observed seasonal variation in NH_3 VCDs. This result is not surprising, given the extremely low levels of fertilizer use in sub-Saharan Africa (FAO, 2020; Hazell & Wood, 2008; Morris et al., 2007). However, the peak NH_3 VCDs during the first half of the rainy season—which we have attributed to seasonal increases in soil and biomass burning emissions—occur at roughly the same time that some fertilizer emissions may be expected to occur, and it is possible that inorganic and organic fertilizer use contributes to the seasonal signal. With efforts underway to substantially increase fertilizer use across the continent (AGRA, 2009), in the future fertilizer use may emerge as a more identifiable driver of seasonal variation in NH_3 VCDs in sub-Saharan Africa.

It is possible that seasonal variation in the phase of NH_3 can influence the observed seasonal NH_3 patterns. Long-term surface measurements of both NH_3 and NH_4^+ are largely limited to West African dry savanna and wet savanna ecoregions, but are consistent with our results. In dry savanna sites, monthly surface NH_3 concentrations and dry deposition tend to be positively related to monthly rainfall, but the opposite is generally the case in wet savanna sites, where NH_3 concentrations and dry deposition tend to be positively related to biomass burning emissions (Delon et al., 2012). In Dakar, Senegal and Bamako, Mali, SO_2 did not appear to influence NH_3 seasonality (Adon et al., 2016). In semi-arid Senegal, NH_3 emissions tend to increase through the rainy season, and are positively related to soil moisture and, during the rainy season, to soil temperature (Delon et al., 2019). Analysis using an Earth system model with dynamic aerosols and interactive chemistry suggests that in the Miombo, Southern Mosaic, and equatorial forest ecoregions, seasonal variation in sulfate and particulate phase NH_4^+ closely mirrors the seasonal NH_3 variation, suggesting that NH_3 observations are representative of atmospheric NH_x ($NH_3 + NH_4^+$) concentrations (Figure S10). In the Northern Mosaic and wet savanna ecoregions, modeled sulfate seasonality departs from NH_3 seasonality, but only results in modest differences between NH_3 and NH_x seasonality (Figure S10).

In the Somalia Acacia and dry savanna ecoregions, both simulated sulfate and NH_x depart from NH_3 seasonality. Interpreting these results is difficult: emissions inventories used by Earth system models lack natural soil emissions of NH_3. Natural soil emissions appear to represent the largest source of NH_3 in the Sahel (Hickman et al., 2018), and are known to be positively related to precipitation in dry ecoregions, which would lead to a distinct seasonality (Hickman et al., 2018; Soper et al., 2016). Our results suggesting that temperature and precipitation are important drivers of NH_3 seasonality in the dry savanna are consistent with these earlier studies, but additional studies incorporating observations of both NH_4^+ and NH_3 seasonality will be needed to confirm our results. In Somalia Acacia, we observe only a weak relationship between precipitation and NH_3 seasonality; model results suggest that NH_x seasonality may be highly dependent on seasonal variation in SO_4 and NH_4^+ (Figure S10). There are no large sources of SO_2 in the Somalia Acacia ecoregion, but SO_4 concentrations may be influenced by anthropogenic emissions from the Middle East, which are substantial (Lee et al., 2011). Sulfate tends to reach its seasonal maximum in July and August in North Africa and the Middle East (Eltahan et al., 2019) (Eltahan et al., 2019), which is also when maxima are observed over Somalia Acacia in ModelE. However, as with the dry savanna, additional surface observations are needed to better understand the causes of seasonal variation in NH_3 concentrations in the ecoregion.

3.3. Summary and Conclusion

With the exception of South Africa and coastal regions of North Africa, fossil fuel emissions and fertilizer use across Africa has remained below—sometimes far below—levels found in other parts of the world during the early 21st century. As a consequence, emissions from soils (including animal excreta) and biomass burning remain the primary sources of atmospheric NO_2 as well as of NH_3, so seasonal variation in the factors that influence these emissions can be expected to be important determinants of their concentrations in the atmosphere. NO_x and NH_3 may originate from similar sources, but differences in the specific processes

producing each gas, as well as in the relative importance of different sources, result in large scale differences in the seasonal variation of both gases. Our analyses reveal that in dry ecoregions, variation in soil emissions is the primary determinant of seasonality in trace N gas VCDs. In mesic ecoregions with a distinct rainy and dry season, we find that seasonal changes in biomass burning emissions determine the seasonality of NO_2 VCDs, but seasonal changes in multiple sources are responsible for NH_3 seasonality in mesic ecoregions.

Specifically, we find that precipitation is a proximate and ultimate driver of the NO_2 seasonality regime. In dry regions, below a precipitation threshold of 500 mm yr^{-1}, NO_2 VCDs are positively related to monthly precipitation. In more mesic regions with MAP between 500 and 1,750 mm yr^{-1} which still retain distinct rainy and dry seasons, NO_2 VCDs are negatively related to monthly precipitation. This 500–1,750 mm yr^{-1} precipitation range largely defines where biomass burning during the dry season is an important part of the regional ecology. In these relatively mesic ecoregions, NO_2 increases during the dry season, in tandem with increases in burned area, and then declines during the rainy season, when burned area decreases. In ecoregions with MAP below 500 mm yr^{-1}—where biomass burning is not widespread—precipitation exerts a more direct control on NO_2 VCDs through its effects on soil N cycling. During the dry season, low precipitation limits biogenic activity, and NO_2 VCDs are low. But at the beginning of the rainy season, precipitation induces large pulses of NO emissions from soils, causing NO_2 VCDs to increase; NO_2 VCDs remain elevated during the rainy season as precipitation sustains biogenic activity in soils.

The division into dry and mesic ecoregions is also an important determinant of NH_3 seasonality and its drivers. In dry ecoregions with less than 500 mm precipitation yr^{-1}, NH_3 VCDs increase during the rainy season, and are low during the dry season. In these regions, temperature and precipitation appear to be the primary controls over seasonal variation in NH_3 VCDs, pointing to variation in soil emissions—including from livestock excreta—as the main cause of seasonality. In mesic ecoregions with distinct rainy and dry seasons, NH_3 VCDs peaked toward the end of the dry season, lagging 1–2 months behind the peak in NO_2 emissions and biomass burning. In the northern mesic ecoregions, temperature explains most of the variation in NH_3 VCDs, but CO VCDs can also be a significant predictor. As with the dry ecoregions, the importance of temperature as a predictor suggests that emissions from soils and livestock excreta are the critical drivers of seasonality in the northern mesic ecoregions, where livestock densities are much higher than in the southern mesic ecoregions. In the southern mesic regions, CO VCDs explain more variation than temperature, which is a weak or insignificant predictor of NH_3 seasonality. The importance of CO as a predictor variable suggests that emissions from burning of woody fuel—which is much more widespread in the southern biomass burning region—or smoldering fires toward the end of the burning season may have contributed to the lagged NH_3 seasonality in these southern mesic ecoregions (van der Werf et al., 2006; Whitburn et al., 2015).

In line with low rates of fertilizer use in sub-Saharan Africa, our analyses do not provide clear support for an important contribution of NH_3 from fertilizer applications. The use of fertilizers would be expected to contribute to an increase in NH_3 VCDs after the start of the rainy season, while we find that NH_3 VCDs are elevated prior to that. But as efforts to increase fertilizer use by 1–2 orders of magnitude take hold across the continent (International Fertilizer Association, 2017; Toenniessen et al., 2008), we may expect early rainy season NH_3 concentrations to increase as well. And although precipitation and biomass burning are currently the most important drivers of NO_2 seasonality, projections suggest a rapid increase in fossil fuel combustion will occur in sub-Saharan Africa, contributing to an equally rapid rise in NO_x emissions (Liousse et al., 2014). At the same time as the fertilizer and fossil fuel use is increasing, biomass burning regions in Africa are in the midst of a decline in burned area (Andela & van der werf, 2014; Andela et al., 2017), which has led to a decline in related NO_x emissions (Hickman et al., 2021). These countering trends could result in a reduction in the amplitude of NO_2 seasonality in the coming decades, particularly in biomass burning regions. In the future, the sources and amplitude of seasonal variation in atmospheric NO_2 and NH_3 concentrations over Africa may be substantially modified by changing anthropogenic activities.

Our study does not provide inverse estimates of emissions or apportion sources, and so does not provide a direct check on modeled emission estimates. However, our evaluation of ecoregion-specific seasonality and first-order relationships to MAP may provide a useful check for global models that dynamically simulate NO_x and NH_3 emissions. The insights provided into how emission regimes vary by ecoregion may further provide hints as to why models may fail to match observations or the sources of model bias—for example,

by testing the relative importance of biomass burning and soil emissions and their seasonal responses to environmental drivers and atmospheric conditions.

Data Availability Statement

All data used in this study are available from public sources. The IASI-NH_3 data are available from the IASI https://iasi.aeris–data.fr/nh3/. GHCN Gridded V2 data were provided by the NOAA/OAR/ESRL PSD, Boulder, Colorado, USA, from their Web site at https://www.esrl.noaa.gov/psd/. GFED4s biomass burning emissions of NH_3 and NO_2, as well as MODIS burned area data, are available from https://www.globalfiredata.org/data.html, OMI NO_2 data are available from https://disc.gsfc.nasa.gov/datasets/OMNO2d_V003/summary, TRMM 3B42 precipitation data are available from https://pmm.nasa.gov/data-access/downloads/trmm, and TNC ecoregions are available from http://maps.tnc.org/gis_data.html.

Acknowledgments
Jonathan E. Hickman's research was supported by an appointment to the NASA Postdoctoral Program at the Goddard Institute for Space Studies, administered by Universities Space Research Association under contract with NASA.

References

Adon, M., Galy-Lacaux, C., Yoboué, V., Delon, C., Lacaux, J. P., Castera, P., et al. (2010). Long term measurements of sulfur dioxide, nitrogen dioxide, ammonia, nitric acid and ozone in Africa using passive samplers. *Atmospheric Chemistry and Physics*, *10*(15), 7467–7487. https://doi.org/10.5194/acp-10-7467-2010

Adon, M., Yoboué, V., Galy-Lacaux, C., Liousse, C., Diop, B., Doumbia, E. H. T., et al. (2016). Measurements of NO_2, SO_2, NH_3, HNO_3 and O_3 in West African urban environments. *Atmospheric Environment*, *135*(2), 31–40. https://doi.org/10.1016/j.atmosenv.2016.03.050

AGRA. (2009). *AGRA in 2008: Building on the new momentum in African agriculture*.

Akagi, S. K., Yokelson, R. J., Wiedinmyer, C., Alvarado, M. J., Reid, J. S., Karl, T., et al. (2011). Emission factors for open and domestic biomass burning for use in atmospheric models. *Atmospheric Chemistry and Physics*, *11*(9), 4039–4072. https://doi.org/10.5194/acp-11-4039-2011

Al-Kanani, T., MacKenzie, A., & Barthakur, N. (1991). Soil water and ammonia volatilization relationships with surface-applied nitrogen fertilizer solutions. *Soil Science Society of America Journal*, *55*, 1761–1766. https://doi.org/10.2136/sssaj1991.03615995005500060043x

Andela, N., Morton, D. C., Giglio, L., Chen, Y., Van Der Werf, G. R., Kasibhatla, P. S., et al. (2017). A human-driven decline in global burned area. *Science*, *356*(6345), 1356–1362. https://doi.org/10.1126/science.aal4108

Andela, N., & van der werf, G. R. (2014). Recent trends in African fires driven by cropland expansion and El Niño to la Niña transition. *Nature Climate Change*, *4*(9), 791–795. https://doi.org/10.1038/nclimate2313

Balasubramanian, S., Koloutsou-Vakakis, S., McFarland, D. M., & Rood, M. J. (2015). Reconsidering emissions of ammonia from chemical fertilizer usage in Midwest USA. *Journal of Geophysical Research: Atmospheres*, *120*, 6232–6246. https://doi.org/10.1002/2014JD021636

Bauer, S. E., Tsigaridis, K., & Miller, R. (2016). Significant atmospheric aerosol pollution caused by world food cultivation. *Geophysical Research Letters*, *43*(10), 5394–5400. https://doi.org/10.1002/2016GL068354

Behera, S. N., Sharma, M., Aneja, V. P., & Balasubramanian, R. (2013). Ammonia in the atmosphere: A review on emission sources, atmospheric chemistry and deposition on terrestrial bodies. *Environmental Science and Pollution Research*, *20*, 8092–8131. https://doi.org/10.1007/s11356-013-2051-9

Birch, H. F. (1958). The effect of soil drying on humus decomposition and nitrogen availability. *Plant and Soil*, *10*(1), 9–31. https://doi.org/10.1007/bf01343734

Birch, H. F. (1960). Nitrification in soils after different periods of dryness. *Plant and Soil*, *12*(1), 81–96. https://doi.org/10.1007/BF01377763

Bouwman, A. F., Heuberger, P. S. C., Van Drecht, G., Van Der Hoek, K. W., & Beusen, A. H. W. (2008). Bottom-up uncertainty estimates of global ammonia emissions from global agricultural production systems. *Atmospheric Environment*, *42*(24), 6067–6077. https://doi.org/10.1016/j.atmosenv.2008.03.044

Bouwman, A. F., Lee, D. S., Asman, W. A. H., Dentener, F. J., Van Der Hoek, K. W., & Olivier, J. G. J. (1997). A global high-resolution emission inventory for ammonia. *Global Biogeochemical Cycles*, *11*(4), 561–587. https://doi.org/10.1029/97gb02266

Cahoon, D. R., Stocks, B. J., Levine, J. S., Cofer, W. R., & O'Neill, K. P. (1992). Seasonal distribution of African savanna fires. *Nature*, *359*(6398), 812–815. https://doi.org/10.1038/359812a0

Celarier, E. A., Brinksma, E. J., Gleason, J. F., Veerkind, J. P., Cede, A., Herman, J. R., et al. (2008). Validation of ozone monitoring instrument nitrogen dioxide columns. *Journal of Geophysical Research*, *113*(15), D15S15. https://doi.org/10.1029/2007JD008908

Chen, L.-W. A., Verburg, P., Shackelford, A., Zhu, D., Susfalk, R., Chow, J. C., & Watson, J. G. (2010). Moisture effects on carbon and nitrogen emission from burning of wildland biomass. *Atmospheric Chemistry and Physics*, *10*(14), 6617–6625. https://doi.org/10.5194/acp-10-6617-2010

Clarisse, L., Clerbaux, C., Dentener, F., Hurtmans, D., & Coheur, P. F. (2009). Global ammonia distribution derived from infrared satellite observations. *Nature Geoscience*, *2*(7), 479–483. https://doi.org/10.1038/ngeo551

Clarisse, L., Van Damme, M., Gardner, W., Coheur, P.-F., Clerbaux, C., Whitburn, S., et al. (2019). Atmospheric ammonia (NH_3) emanations from Lake Natron's saline mudflats. *Scientific Reports*, *9*, 4441. https://doi.org/10.1038/s41598-019-39935-3

Dammers, E., Mclinden, C. A., Griffin, D., Shephard, M. W., Van Der Graaf, S., Lutsch, E., et al. (2019). NH_3 emissions from large point sources derived from CrIS and IASI satellite observations. *Atmospheric Chemistry and Physics Discussions*, *19*, 12261–12293.

Dammers, E., Shephard, M. W., Palm, M., Cady-Pereira, K., Capps, S., Lutsch, E., et al. (2017). Validation of the CrIS fast physical NH_3 retrieval with ground-based FTIR. *Atmospheric Measurement Techniques*, *10*(7), 2645–2667. https://doi.org/10.5194/amt-10-2645-2017

Davidson, E. A. (1992). Pulses of nitric oxide and nitrous oxide flux following wetting of dry soil: An assessment of probable sources and importance relative to annual fluxes. *Ecological Bulletins*, *42*, 149–155.

Davidson, E. A., Matson, P. A., Vitousek, P. M., Riley, R., Dunkin, K., Garcia-Mendez, G., & Maass, J. M. (1993). Processes regulating soil emissions of NO and N_2O in a seasonally dry tropical forest. *Ecology*, *74*(1), 130–139. https://doi.org/10.2307/1939508

Davidson, E. A., & Verchot, L. V. (2000). Testing the hole-in-the-pipe model of nitric and nitrous oxide emissions from soils using the TRAGNET database. *Global Biogeochemical Cycles*, *14*(4), 1035–1043. https://doi.org/10.1029/1999GB001223

Davidson, E. A., Vitousek, P. M., Matson, P. A., Riley, R., García-Méndez, G., & Maass, J. M. (1991). Soil emissions of nitric oxide in a seasonally dry tropical forest of México. *Journal of Geophysical Research*, *96*(D8), 15439–15445. https://doi.org/10.1029/91JD01476

Delon, C., Galy-Lacaux, C., Adon, M., Liousse, C., Serça, D., Diop, B., & Akpo, A. (2012). Nitrogen compounds emission and deposition in West African ecosystems: Comparison between wet and dry savanna. *Biogeosciences*, *9*(1), 385–402. https://doi.org/10.5194/bg-9-385-2012

Delon, C., Galy-Lacaux, C., Boone, A., Liousse, C., Serça, D., Adon, M., et al. (2010). Atmospheric nitrogen budget in Sahelian dry savannas. *Atmospheric Chemistry and Physics*, *10*(6), 2691–2708. https://doi.org/10.5194/acp-10-2691-2010

Delon, C., Galy-Lacaux, C., Serça, D., Personne, E., Mougin, E., Adon, M., et al. (2019). Modelling land–atmosphere daily exchanges of NO, NH_3, and CO_2 in a semi-arid grazed ecosystem in Senegal. *Biogeosciences*, *16*(9), 2049–2077. https://doi.org/10.5194/bg-16-2049-2019

Denier Van Der Gon, H., & Bleeker, A. (2005). Indirect N_2O emission due to atmospheric N deposition for the Netherlands. *Atmospheric Environment*, *39*(32), 5827–5838. https://doi.org/10.1016/j.atmosenv.2005.06.019

Dick, J., Skiba, U., & Wilson, J. (2001). The effect of rainfall on NO and N_2O emissions from Ugandan agroforest soils. *Phyton*, *41*, 73–80.

Edwards, D. P., Emmons, L. K., Gille, J. C., Chu, A., Attié, J. L., Giglio, L., et al. (2006). Satellite-observed pollution from Southern Hemisphere biomass burning. *Journal of Geophysical Research*, *111*(14), D14312. https://doi.org/10.1029/2005JD006655

Eltahan, M., Magooda, M., & Alahmadi, S. (2019). Spatiotemporal assessment of SO_2, SO_4 and AOD from over MENA domain from 2006–2016 using multiple satellite and reanalysis MERRA-2 data. *Journal of Geoscience and Environment Protection*, *7*(4), 156–174. https://doi.org/10.4236/gep.2019.74010

Fan, Y., & van den Dool, H. (2008). A global monthly land surface air temperature analysis for 1948–present. *Journal of Geophysical Research*, *113*(1), D01103. https://doi.org/10.1029/2007JD008470

FAO. (2020). *FAO Statistics database*. Retrieved from http://www.fao.org/faostat/en/

Feig, G. T., Mamtimin, B., & Meixner, F. X. (2008). Soil biogenic emissions of nitric oxide from a semi-arid savanna in South Africa. *Biogeosciences*, *5*(6), 1723–1738. https://doi.org/10.5194/bg-5-1723-2008

Galy-Lacaux, C., & Delon, C. (2014). Nitrogen emission and deposition budget in West and Central Africa. *Environmental Research Letters*, *9*(12), 125002. https://doi.org/10.1088/1748-9326/9/12/125002

Galy-Lacaux, C., & Modi, A. I. (1998). Precipitation chemistry in the Sahelian savanna of Niger, Africa. *Journal of Atmospheric Chemistry*, *30*(3), 319–343. https://doi.org/10.1023/A:1006027730377

Ghude, S. D., Fadnavis, S., Beig, G., Polade, S. D., & van der, A. R. J. (2008). Detection of surface emission hot spots, trends, and seasonal cycle from satellite-retrieved NO_2 over India. *Journal of Geophysical Research*, *113*(20). https://doi.org/10.1029/2007JD009615

Giglio, L., Boschetti, L., Roy, D. P., Humber, M. L., & Justice, C. O. (2018). The Collection 6 MODIS burned area mapping algorithm and product. *Remote Sensing of Environment*, *217*, 72–85. https://doi.org/10.1016/j.rse.2018.08.005

Giglio, L., Randerson, J. T., & Van Der Werf, G. R. (2013). Analysis of daily, monthly, and annual burned area using the fourth-generation global fire emissions database (GFED4). *Journal of Geophysical Research: Biogeosciences*, *118*(1), 317–328. https://doi.org/10.1002/jgrg.20042

Goode, J. G., Yokelson, R. J., Susott, R. A., & Ward, D. E. (1999). Trace gas emissions from laboratory biomass fires measured by open-path Fourier transform infrared spectroscopy. *Journal of Chemical Information and Modeling*, *104*(D17), 21237–21245. https://doi.org/10.1029/1999jd900360

Guntiñas, M. E., Leirós, M. C., Trasar-Cepeda, C., & Gil-Sotres, F. (2012). Effects of moisture and temperature on net soil nitrogen mineralization: A laboratory study. *European Journal of Soil Biology*, *48*, 73–80. https://doi.org/10.1016/j.ejsobi.2011.07.015

Hazell, P., & Wood, S. (2008). Drivers of change in global agriculture. *Philosophical Transactions of the Royal Society B: Biological Sciences*, *363*(1491), 495–515. https://doi.org/10.1098/rstb.2007.2166

Hickman, J. E., Andela, N., Dammers, E., Clarisse, L., Coheur, P.-F., Van Damme, M., et al. (2020). Changes in biomass burning, wetland extent, or agriculture drive atmospheric NH_3 trends in several African regions. *Atmospheric Chemistry and Physics Discussions*, 1–33. https://doi.org/10.5194/acp-2020-945

Hickman, J. E., Andela, N., Tsigaridis, K., Galy-Lacaux, C., Ossohou, M., & Bauer, S. E. (2021). Reductions in NO_2 burden over north equatorial Africa from decline in biomass burning in spite of growing fossil fuel use, 2005 to 2017. *Proceedings of the National Academy of Sciences of the United States of America*, *118*(7), e2002579118. https://doi.org/10.1073/pnas.2002579118

Hickman, J. E., Dammers, E., Galy-Lacaux, C., & Van Der Werf, G. R. (2018). Satellite evidence of substantial rain-induced soil emissions of ammonia across the Sahel. *Atmospheric Chemistry and Physics*, *18*(22), 16713–16727. https://doi.org/10.5194/acp-18-16713-2018

Hickman, J. E., Huang, Y., Wu, S., Diru, W., Groffman, P. M., Tully, K. L., & Palm, C. A. (2017). Nonlinear response of nitric oxide fluxes to fertilizer inputs and the impacts of agricultural intensification on tropospheric ozone pollution in Kenya. *Global Change Biology*, *23*(8), 3193–3204. https://doi.org/10.1111/gcb.13644

Hirota, M., Holmgren, M., Van Nes, E. H., & Scheffer, M. (2011). Global resilience of tropical forest. *Science*, *334*, 232–235. https://doi.org/10.1126/science.1210657

Hoesly, R. M., Smith, S. J., Feng, L., Klimont, Z., Janssens-Maenhout, G., Pitkanen, T., et al. (2017). Historical (1750–2014) anthropogenic emissions of reactive gases and aerosols from the Community Emission Data System (CEDS). *Geoscientific Model Development Discussions*, *11*, 369–408. https://doi.org/10.5194/gmd-2017-43

Hudman, R. C., Moore, N. E., Mebust, A. K., Martin, R. V., Russell, A. R., Valin, L. C., & Cohen, R. C. (2012). Steps towards a mechanistic model of global soil nitric oxide emissions: Implementation and space based-constraints. *Atmospheric Chemistry and Physics*, *12*(16), 7779–7795. https://doi.org/10.5194/acp-12-7779-2012

Huffman, G. J., Adler, R. F., Bolvin, D. T., Gu, G., Nelkin, E. J., Bowman, K. P., et al. (2007). The TRMM multisatellite precipitation analysis (TMPA): Quasi-global, multiyear, combined-sensor precipitation estimates at fine scales. *Journal of Hydrometeorology*, *8*(1), 38–55. https://doi.org/10.1175/jhm560.1

Hurtmans, D., Coheur, P. F., Wespes, C., Clarisse, L., Scharf, O., Clerbaux, C., et al. (2012). FORLI radiative transfer and retrieval code for IASI. *Journal of Quantitative Spectroscopy and Radiative Transfer*, *113*(11), 1391–1408. https://doi.org/10.1016/j.jqsrt.2012.02.036

International Fertilizer Association. (2017). *Fertilizer outlook 2017–2021*. https://doi.org/10.1021/ic034060s

Jacob, D. J. (1999). *Introduction to atmospheric chemistry*. Princeton University Press.

Jaeglé, L., Martin, R. V., Chance, K., Steinberger, L., Kurosu, T. P., Jacob, D. J., et al. (2004). Satellite mapping of rain-induced nitric oxide emissions from soils. *Journal of Geophysical Research*, *109*(21). https://doi.org/10.1029/2004JD004787

Jaeglé, L., Steinberger, L., Martin, R. V., & Chance, K. (2005). Global partitioning of NOx sources using satellite observations: Relative roles of fossil fuel combustion, biomass burning and soil emissions. *Faraday Discussions*, *130*, 407. https://doi.org/10.1039/b502128f

Kniveton, D. R., Layberry, R., Williams, C. J. R., & Peck, M. (2009). Trends in the start of the wet season over Africa. *International Journal of Climatology*, *29*, 1216–1225. https://doi.org/10.1002/joc10.1002/joc.1792

Krawchuk, M. A., Moritz, M. A., Parisien, M. A., Van Dorn, J., & Hayhoe, K. (2009). Global pyrogeography: The current and future distribution of wildfire. *PLoS ONE*, *4*(4), e5102. https://doi.org/10.1371/journal.pone.0005102

Krotkov, N. A., Lamsal, L. N., Celarier, E. A., Swartz, W. H., Marchenko, S. V., Bucsela, E. J., et al. (2017). The version 3 OMI NO_2 standard product. *Atmospheric Measurement Techniques Discussions*, *10*(2), 3133–3149. https://doi.org/10.5194/amt-2017-44

Krupa, S. V. (2003). Effects of atmospheric ammonia (NH_3) on terrestrial vegetation: A review. *Environmental Pollution*, *124*(2), 179–221. https://doi.org/10.1016/S0269-7491(02)00434-7

Lamsal, L. N., Krotkov, N. A., Celarier, E. A., Swartz, W. H., Pickering, K. E., Bucsela, E. J., et al. (2014). Evaluation of OMI operational standard NO_2 column retrievals using in situ and surface-based NO_2 observations. *Atmospheric Chemistry and Physics*, *14*(21), 11587–11609. https://doi.org/10.5194/acp-14-11587-2014

Lee, C., Martin, R. V., Van Donkelaar, A., Lee, H., Dickerson, R. R., Hains, J. C., et al. (2011). SO_2 emissions and lifetimes: Estimates from inverse modeling using in situ and global, space-based (SCIAMACHY and OMI) observations. *Journal of Geophysical Research*, *116*(6), 1–13. https://doi.org/10.1029/2010JD014758

Lelieveld, J., Evans, J. S., Fnais, M., Giannadaki, D., & Pozzer, A. (2015). The contribution of outdoor air pollution sources to premature mortality on a global scale. *Nature*, *525*(7569), 367–371. https://doi.org/10.1038/nature15371

Liousse, C., Assamoi, E., Criqui, P., Granier, C., & Rosset, R. (2014). Explosive growth in African combustion emissions from 2005 to 2030. *Environmental Research Letters*, *9*(3), 035003. https://doi.org/10.1088/1748-9326/9/3/035003

Martins, J. J., Dhammapala, R. S., Lachmann, G., Galy-Lacaux, C., & Pienaar, J. J. (2007). Long-term measurements of sulphur dioxide, nitrogen dioxide, ammonia, nitric acid and ozone in southern Africa using passive samplers. *South African Journal of Science*, *103*(7–8), 336–342. https://doi.org/10.5194/acpd-10-4407-2010

Masso, C., Nziguheba, G., Mtutegi, J., Galy-Lacaux, C., Wendt, K., Butterbach-Bahl, K., et al. (2017). Soil fertility management in sub-Saharan Africa. In E. Lichtfouse (Ed.), *Sustainable agriculture reviews* (p. 304). Springer International Publishing.

Matson, P. A., McDowell, W. H., Townsend, A. R., Vitousek, P. M., & Vitousek, P. M. (1999). The globalization of N deposition: Ecosystem consequences in tropical environments. *Biogeochemistry*, *46*, 67–83. https://doi.org/10.1007/bf01007574

McLinden, C. A., Fioletov, V., Boersma, K. F., Kharol, S. K., Krotkov, N., Lamsal, L., et al. (2014). Improved satellite retrievals of NO_2 and SO_2 over the Canadian oil sands and comparisons with surface measurements. *Atmospheric Chemistry and Physics*, *14*(7), 3637–3656. https://doi.org/10.5194/acp-14-3637-2014

Mebust, A. K., & Cohen, R. C. (2013). Observations of a seasonal cycle in NOx emissions from fires in African woody savannas. *Geophysical Research Letters*, *40*(7), 1451–1455. https://doi.org/10.1002/grl.50343

Meixner, F. X., Fickinger, T., Marufu, L., Ser, D., Nathaus, F. J., Makina, E., et al. (1997). Preliminary results on nitric oxide emission from a southern African savanna ecosystem. *Nutrient Cycling in Agroecosystems*, *48*, 123–138. https://doi.org/10.1023/a:1009765510538

Morris, M., Kelly, V., Kopicki, R., & Byerlee, D. (2007). Fertilizer use in African agriculture: Lessons learned and good practice guidelines (Vol. 44). Experimental Agriculture. https://doi.org/10.1017/S0014479707005777

Nicholson, S., Some, B., McCollum, J., Nelkin, E., Klotter, D., Berte, Y., et al. (2003). Validation of TRMM and other rainfall estimates with a high-density gauge dataset for West Africa. Part II: Validation of TRMM rainfall products. *Journal of Applied Meteorology*, *42*, 1355–1368. https://doi.org/10.1175/1520-0450(2003)042<1355:votaor>2.0.co;2

Olivier, J. G. J., Bouwman, A. F., Van Der Hoek, K. W., & Berdowski, J. J. M. (1998). Global air emission inventories for anthropogenic sources of NO(x), NH_3 and N_2O in 1990. *Environmental Pollution*, *102*(suppl. 1), 135–148. https://doi.org/10.1016/S0269-7491(98)80026-2

Olson, D. M., & Dinerstein, E. (2002). The Global 200: Priority ecoregions for global conservation. *Annals of the Missouri Botanical Garden*, *89*(2), 199–224. https://doi.org/10.2307/3298564

Ossohou, M., Galy-Lacaux, C., Yoboué, V., Hickman, J. E., Gardrat, E., Adon, M., et al. (2019). Trends and seasonal variability of atmospheric NO_2 and HNO_3 concentrations across three major African biomes inferred from long-term series of ground-based and satellite measurements. *Atmospheric Environment*, *207*, 148–166. https://doi.org/10.1016/j.atmosenv.2019.03.027

Otter, L. B., Yang, W. X., Scholes, M. C., & Meixner, F. X. (1999). Nitric oxide emissions from a southern African savanna. *Journal of Geophysical Research*, *104*, 18471–18485. https://doi.org/10.1029/1999jd900148

Paul, B. K., Frelat, R., Birnholz, C., Ebong, C., Gahigi, A., Groot, J. C. J., et al. (2017). Agricultural intensification scenarios, household food availability and greenhouse gas emissions in Rwanda: Ex-ante impacts and trade-offs. *Agricultural Systems*, *163*, 16–26. https://doi.org/10.1016/j.agsy.2017.02.007

Paul, E. A., & Clark, F. E. (1996). *Soil microbiology and biochemistry* (2nd ed.). Academic Press.

Pilegaard, K. (2013). Processes regulating nitric oxide emissions from soils Processes regulating nitric oxide emissions from soils. *Philosophical Transactions of the Royal Society B: Biological Sciences*, *368*, 20130126. https://doi.org/10.1098/rstb.2013.0126

Placella, S. A., Brodie, E. L., & Firestone, M. K. (2012). Rainfall-induced carbon dioxide pulses result from sequential resuscitation of phylogenetically clustered microbial groups. *Proceedings of the National Academy of Sciences of the United States of America*, *109*(27), 10931–10936. https://doi.org/10.1073/pnas.1204306109

Pope, A., Burnett, R., Thun, M., EE, C., D, K., I, K., & GD, T. (2002). Long-term exposure to fine particulate air pollution. *Journal of the American Medical Association*, *287*(9), 1132–1141. https://doi.org/10.1001/jama.287.9.1132

Potter, S., Randerson, T., Field, B., Matson, A., Vitousek, P. M., Mooney, H. A., & Klooster, S. A. (1993). Terrestrial ecosystem production: A process model based on global satellite and surface data. *Global Biogeochemical Cycles*, *7*(4), 811–841. https://doi.org/10.1029/93gb02725

Ramo, R., Roteta, E., Bistinas, I., van Wees, D., Bastarrika, A., Chuvieco, E., & van der Werf, G. R. (2021). African burned area and fire carbon emissions are strongly impacted by small fires undetected by coarse resolution satellite data. *Proceedings of the National Academy of Sciences of the United States of America*, *118*(9), 1–7. https://doi.org/10.1073/pnas.2011160118

Randerson, J. T., Chen, Y., Van Der Werf, G. R., Rogers, B. M., & Morton, D. C. (2012). Global burned area and biomass burning emissions from small fires. *Journal of Geophysical Research*, *117*(4), G04012. https://doi.org/10.1029/2012JG002128

Reich, P. B., Peterson, D. W., Wedin, D. A., & Wrage, K. (2001). Fire and vegetation effects on productivity and nitrogen cycling across a forest-grassland continuum. *Ecology*, *82*(6), 1703–1719. https://doi.org/10.1890/0012-9658(2001)082[1703:faveop]2.0.co;2

Roberts, G., Wooster, M. J., Xu, W., & He, J. (2018). Fire activity and fuel consumption dynamics in sub-Saharan Africa. *Remote Sensing*, *10*(10), 1591. https://doi.org/10.3390/rs10101591

Robinson, T. P., Wint, G. R. W., Conchedda, G., Van Boeckel, T. P., Ercoli, V., Palamara, E., et al. (2014). Mapping the global distribution of livestock. *PLoS ONE*, *9*(5), e96084. https://doi.org/10.1371/journal.pone.0096084

Roteta, E., Bastarrika, A., Padilla, M., Storm, T., & Chuvieco, E. (2019). Development of a Sentinel-2 burned area algorithm: Generation of a small fire database for sub-Saharan Africa. *Remote Sensing of Environment*, *222*, 1–17. https://doi.org/10.1016/j.rse.2018.12.011

Rufino, M. C., Brandt, P., Herrero, M., & Butterbach-Bahl, K. (2014). Reducing uncertainty in nitrogen budgets for African livestock systems. *Environmental Research Letters*, *9*(10), 105008. https://doi.org/10.1088/1748-9326/9/10/105008

Rufino, M. C., Rowe, E. C., Delve, R. J., & Giller, K. E. (2006). Nitrogen cycling efficiencies through resource-poor African crop-livestock systems. *Agriculture, Ecosystems & Environment*, *112*(4), 261–282. https://doi.org/10.1016/j.agee.2005.08.028

Saad, O. A. L. O., & Conrad, R. (1993). Temperature dependence of nitrification, denitrification, and turnover of nitric oxide in different soils. *Biology and Fertility of Soils*, *15*(1), 21–27. https://doi.org/10.1007/BF00336283

Sahrawat, K. L. (1984). Effects of temperature and moisture on urease activity in semi-arid tropical soils. *Plant and Soil*, *8*(288), 401–408. https://doi.org/10.1007/BF02450373

Schlecht, E., & Hiernaux, P. (2004). Beyond adding up inputs and outputs: Process assessment and upscaling in modelling nutrient flows N. *Nutrient Cycling in Agroecosystems*, *70*, 303–319. https://doi.org/10.1007/s10705-004-0765-2

Schlecht, E., Hiernaux, P., Kadaouré, I., Hülsebusch, C., & Mahler, F. (2006). A spatio-temporal analysis of forage availability and grazing and excretion behaviour of herded and free grazing cattle, sheep and goats in Western Niger. *Agriculture, Ecosystems & Environment*, *113*(1–4), 226–242. https://doi.org/10.1016/j.agee.2005.09.008

Seifert, J. (1980). Effect of temperature on nitrification intensity in soil. *Folia Microbiologica*, *25*(2), 144–147. https://doi.org/10.1007/BF02933014

Seinfeld, J. H., & Pandis, S. N. (2016). *Atmospheric chemistry and physics: From air pollution to climate change* (3rd ed.). John Wiley and Sons.

Serça, D., Delmas, R., Le Roux, X., Parsons, D. A. B., Scholes, M. C., Abbadie, L., et al. (1998). Comparison of nitrogen monoxide emissions from several African tropical ecosystems and influence of season and fire. *Global Biogeochemical Cycles*, *12*(4), 637–651. https://doi.org/10.1029/98GB02737

Serneels, S., & Lambin, E. (2001). Impact of land-use changes on the wildebeest migration in the northern part of the Serengeti-Mara ecosystem related records. *Journal of Biogeography*, *28*, 391–407.

Silva, R. A., West, J. J., Zhang, Y., Anenberg, S. C., Lamarque, J. F., Shindell, D. T., et al. (2013). Global premature mortality due to anthropogenic outdoor air pollution and the contribution of past climate change. *Environmental Research Letters*, *8*(3), 034005. https://doi.org/10.1088/1748-9326/8/3/034005

Sinha, P., Hobbs, P. V., Yokelson, R. J., Blake, D. R., Gao, S., & Kirchstetter, T. W. (2004). Emissions from Miombo woodland and dambo grassland savanna fires. *Journal of Geophysical Research*, *109*(11), D11305. https://doi.org/10.1029/2004JD004521

Sommer, S. G., Schjoerring, J. K., & Denmead, O. T. (2004). Ammonia emission from mineral fertilizers and fertilized crops. *Advances in Agronomy*, *82*, 557–622. https://doi.org/10.1016/s0065-2113(03)82008-4

Soper, F. M., Boutton, T. W., Groffman, P. M., & Sparks, J. P. (2016). Nitrogen trace gas fluxes from a semiarid subtropical savanna under woody legume encroachment. *Global Biogeochemical Cycles*, *30*, 614–628. https://doi.org/10.1002/2015gb005298

Stevens, C. J., David, T. I., & Storkey, J. (2018). Atmospheric nitrogen deposition in terrestrial ecosystems: Its impact on plant communities and consequences across trophic levels. *Functional Ecology*, *32*(7), 1757–1769. https://doi.org/10.1111/1365-2435.13063

Sutton, M. A., Reis, S., Riddick, S. N., Dragosits, U., Nemitz, E., Theobald, M. R., et al. (2013). Towards a climate-dependent paradigm of ammonia emission and deposition. *Philosophical Transactions of the Royal Society B: Biological Sciences*, *368*(1621), 20130166. https://doi.org/10.1098/rstb.2013.0166

Tian, D., & Niu, S. (2015). A global analysis of soil acidification caused by nitrogen addition. *Environmental Research Letters*, *10*(2), 024019. https://doi.org/10.1088/1748-9326/10/2/024019

Toenniessen, G., Adesina, A., & DeVries, J. (2008). Building an alliance for a Green Revolution in Africa. *Annals of the New York Academy of Sciences*, *1136*, 233–242. https://doi.org/10.1196/annals.1425.028

Van Damme, M., Clarisse, L., Heald, C. L., Hurtmans, D., Ngadi, Y., Clerbaux, C., et al. (2014). Global distributions, time series and error characterization of atmospheric ammonia NH_3 from IASI satellite observations. *Atmospheric Chemistry and Physics*, *14*(6), 2905–2922. https://doi.org/10.5194/acp-14-2905-2014

Van Damme, M., Whitburn, S., Clarisse, L., Clerbaux, C., Hurtmans, D., & Coheur, P. F. (2017). Version 2 of the IASI NH_3 neural network retrieval algorithm: Near-real-time and reanalysed datasets. *Atmospheric Measurement Techniques*, *10*(12), 4905–4914. https://doi.org/10.5194/amt-10-4905-2017

van der, A. R. J., Eskes, H. J., Boersma, K. F., van Noije, T. P. C., Van Roozendael, M., De Smedt, I., et al. (2008). Trends, seasonal variability and dominant NOx source derived from a ten year record of NO_2 measured from space. *Journal of Geophysical Research*, *113*(4), D04302. https://doi.org/10.1029/2007JD009021

van der Werf, G. R., Guido, R., Randerson, J. T., Giglio, L., van Leeuwen, T. T., Chen, Y., et al. (2017). Global fire emissions estimates during 1997–2016. *Earth System Science Data*, *9*(2), 697–720. https://doi.org/10.5194/essd-9-697-2017

van der Werf, G. R., Randerson, J. T., Giglio, L., Collatz, G. J., Kasibhatla, P. S., & Arellano, A. F. (2006). Interannual variability in global biomass burning emissions from 1997 to 2004. *Atmospheric Chemistry and Physics*, *6*, 3423–3441. https://doi.org/10.5194/acp-6-3423-2006

Vanlauwe, B., & Giller, K. (2006). Popular myths around soil fertility management in sub-Saharan Africa. *Agriculture, Ecosystems & Environment*, *116*(1–2), 34–46. https://doi.org/10.1016/j.agee.2006.03.016

van Leeuwen, T. T., & van der Werf, G. R. (2011). Spatial and temporal variability in the ratio of trace gases emitted from biomass burning. *Atmospheric Chemistry and Physics*, *11*(8), 3611–3629. https://doi.org/10.5194/acp-11-3611-2011

Vitousek, P. M. (2004). *Nutrient cycling and limitation: Hawai'i as a model system*. Princeton University Press.

Vitousek, P. M., Naylor, R., Crews, T., David, M., Drinkwater, L., Holland, E., et al. (2009). Nutrient imbalances in agricultural development. *Science*, *324*, 1519–1520. https://doi.org/10.1126/science.1170261

Whitburn, S., Van Damme, M., Clarisse, L., Bauduin, S., Heald, C. L., Hurtmans, D., et al. (2016). A flexible and robust neural network IASI-NH_3 retrieval algorithm. *Journal of Geophysical Research: Atmospheres*, *3*, 6581–6599. https://doi.org/10.1002/2016JD024828

Whitburn, S., Van Damme, M., Kaiser, J. W., Van Der Werf, G. R., Turquety, S., Hurtmans, D., et al. (2015). Ammonia emissions in tropical biomass burning regions: Comparison between satellite-derived emissions and bottom-up fire inventories. *Atmospheric Environment*, *121*, 42–54. https://doi.org/10.1016/j.atmosenv.2015.03.015

World Bank. (2019). *World Bank open data*. Retrieved from https://www.data.worldbank.org

Yokelson, R. J., Christian, T. J., Karl, T. G., & Guenther, A. (2008). The tropical forest and fire emissions experiment: Laboratory fire measurements and synthesis of campaign. *Revista Internacional de Acupuntura*, *8*, 3509–3527. https://doi.org/10.5194/acp-8-3509-2008

Zheng, B., Chevallier, F., Ciais, P., Yin, Y., & Wang, Y. (2018). On the role of the flaming to smoldering transition in the seasonal cycle of African fire emissions. *Geophysical Research Letters*, *45*(21), 11998–12007. https://doi.org/10.1029/2018GL079092